ARPA ORDER NO. 189-61

MEMORANDUM
RM-4809-ARPA
DECEMBER 1965

DETECTION OF SONAR SINUSOIDS OF UNKNOWN FREQUENCY AND KNOWN OR UNKNOWN PHASE

F. S. Hill, Jr.

PREPARED FOR:

ADVANCED RESEARCH PROJECTS AGENCY

The RAND Corporation
SANTA MONICA • CALIFORNIA

ARPA ORDER NO. 189-61

MEMORANDUM
RM-4809-ARPA
DECEMBER 1965

DETECTION OF SONAR SINUSOIDS OF UNKNOWN FREQUENCY AND KNOWN OR UNKNOWN PHASE

F. S. Hill, Jr.

This research is supported by the Advanced Research Projects Agency under Contract No. SD-79. Any views or conclusions contained in this Memorandum should not be interpreted as representing the official opinion or policy of ARPA.

The RAND Corporation
1700 MAIN ST • SANTA MONICA • CALIFORNIA • 90406

PREFACE

In conjunction with RAND's study of Defense Against Submarine-Launched Ballistic Missiles for the Advanced Research Projects Agency, background investigations of theoretical methods for calculating the performance of nondirectional passive sonobuoys are being conducted. The particular investigation presented in this Memorandum evaluates the performance of a theoretically optimum processor for detecting a sine wave of unknown frequency and unknown phase in gaussian noise.

This study should be of interest to analysts in the fields of sonar and radar as well as to researchers in the general field of signal detection theory.

BLANK PAGE

SUMMARY

This Memorandum considers the problem of detecting a constant sine wave of unknown frequency and amplitude in gaussian noise. In particular, it is assumed that the sinusoid may appear at any one of a finite number of known frequencies, and the probability of its occurrence at each of these frequencies is assumed to be equal. Two cases are treated here. The first assumes that although the frequency is not known, the phase of the signal is known, thus allowing coherent detection. The second acknowledges that the initial phase indeed could not be known, and an analysis of the incoherent detector is made. It is shown that for large output signal-to-noise ratios, the problem in both cases becomes that of detecting one of m approximately orthogonal signals in a noise background. The magnitude of the error in the orthogonality approximation is considered. A physical realization of an approximately optimum detector structure is studied in some detail, and the effect of finite observation time is considered.

The results indicate that the difference between the two cases is small and quite predictable. Thus, in studies of this kind it can be assumed that the initial phase is known, the gaussian character of the quantities that arise may be retained, and finally, the answers can be adjusted to account for the actual lack of knowledge concerning the phase.

BLANK PAGE

ACKNOWLEDGMENTS

The author wishes to express his appreciation to I. S. Blumenthal and F. B. Tuteur (Consultant) of The RAND Corporation for their many helpful discussions that made this work possible. He also wishes to thank M. Blum and P. Swerling (Consultant) of RAND for their careful criticisms and comments in reviewing this Memorandum.

BLANK PAGE

CONTENTS

BLANK PAGE

LIST OF FIGURES

BLANK PAGE

LIST OF SYMBOLS

A	determinant of moment matrix
C	constant of proportionality
d	detection index, $d^2 = P^2T/N_o$
f	frequency of sinusoidal signal, cps
f(x)	probability density functions of random variable x
G(f)	spectral density of noise process at output of a filter, volts^2/cps
H(f)	frequency domain characteristic of a filter
H_i	hypothesis that a sinusoid at i^{th} possible frequency is present in addition to noise
H_o	hypothesis that noise only is present
$h(\tau)$	impulse response of a filter
$I_o(x)$	modified zero-order Bessel function
K, K_1	normalizing constants
$\underline{K}$	covariance matrix of the noise process
k	threshold level
$L(\underline{v}, \theta)$	likelihood ratio given the parameter value θ
$\ell(\underline{v})$	averaged likelihood ratio operating on received signal v(t)
$\underline{M}$	moment matrix
m	number of possible sine wave frequencies
N	noise variance
N(f)	noise power spectral density, volts^2/cps
N_o	noise power spectral density level, volts^2/cps
n	number of samples of v(t) in T sec
n(t)	noise process, volts

P	amplitude of sine wave signal, volts
P_d	detection probability, $P_d = 1 - \beta$
$p(\omega), p(r)$	probability density function of signal frequency ω, r
$Q(x,y)$	$\int_y^\infty t\, e^{-\frac{1}{2}(t^2+x^2)} I_o(xt)dt$, "Q-function"
q	number of observation intervals per year
$R(\tau)$	autocorrelation function of noise process
r_i	envelope of output at time T of narrow-band filter centered at ω_i
$s(t)$	sinusoidal signal waveform
$s_i(t)$	$P \cos(\omega_i t + \theta)$
T	observation time, sec
t	time, sec
$\underline{v}$	vector of uniformly spaced amplitude samples of $n(t)$
$v(t)$	received waveform, volts
x_i	$\log L_i$, processed data
α	probability of false alarm in each observation interval
α^*	a preset allowable value of α
β	probability of false dismissal in each observation interval
$\delta(x)$	Kronecker delta function $\delta(x) = \begin{cases} 1 & x = 0 \\ 0 & x \neq 0 \end{cases}$ Also, Dirac delta function
ϵ	bandwidth parameter of filter
$\theta, \xi, \varphi, \delta$	phase angles of sinusoids, rad
μ_{13}, μ_{14}	moments of gaussian distribution
σ	normalized determinant of moment matrix

$\Phi(x)$	$\frac{1}{\sqrt{2\pi}} \int_{-x}^{x} e^{\frac{-t^2}{2}} dt$, normal probability integral
ψ, ψ_{12}	variances of filter outputs
Ω	frequency band containing all m possible frequencies f_i, cps
ω_i	i^{th} possible sine wave frequency, rad/sec, $\omega_i = 2\pi f_i$

I. INTRODUCTION

The problem considered here is that of detecting the presence of a submarine target by a single, unattended, omnidirectional hydrophone. It is presumed that such a target emits both widebard noise and a set of sine waves of different frequency. This Memorandum considers the detection of the target by means of the sine waves. Since the exact frequency of each sinusoid will not be known in advance, the problem becomes that of detecting one or more sinusoids of unknown frequency in a noise background.

As a first step toward a solution of this problem, the question of detecting a single sinusoid of unknown amplitude and frequency in a background of gaussian noise is considered. The noise is assumed to have a known spectral density and is assumed stationary, at least for the duration of each decision period. In practice, the frequency of the sinusoid may only be known within a band of frequencies, and may, with equal probability, appear anywhere within this band. As a useful approximation to this situation, the assumption is made here that the frequency of the sinusoid has a discrete distribution; that is, it can appear at one of a finite number, m, of possible frequencies. If this assumed number m is large, then the assumption is not greatly different from that of assuming a continuous distribution of frequency over the band of uncertainty.

It is seen later in this Memorandum that the false-alarm rate, being determined only by the noise statistics, is independent of signal amplitude, and that detectability of the target increases monotonically with signal amplitude. Thus, if signal amplitude is

not known, but is known to remain steady over the length of a detection period, then the system threshold is set by the allowable false-alarm rate, and its detection performance will depend only on the actual signal amplitude. Hence, a constant signal amplitude of unknown level can be assumed, as done in this Memorandum, giving final answers in terms of the actual signal amplitude. The signal amplitude may, of course, be converted into target range if the signal level emanating from the target, the transmission loss versus distance and the noise level at the receiver are known.

The first part of the Memorandum deals with the detection of a sinusoid of unknown frequency but known phase in gaussian noise. The known phase assumption is clearly unrealistic if the frequency is not known, but the mathematics are tractable, and it is known from studies of known-frequency sine wave detection that the difference between coherent and incoherent* techniques is small and predictable. The second part demonstrates this, dealing with the detection of sinusoids of both unknown frequency and phase. This study concludes that if work is pursued knowing the phase of the sinusoid, the effect of the actual ignorance of phase may then be included by means of some loss factor which is constant over a large range of situations.

---

*Confusion sometimes arises concerning the terms "coherent" and "incoherent," because their roles in discussions of active radar systems are quite different from their usage here. In radar nomenclature, "coherent" and "incoherent" refer to methods of integrating sequences of pulses, either retaining or destroying the phase structure between different pulses. In the present context, however, there are no pulses at all. Here, "coherent" specifies actual knowledge of signal phase relative to some reference, for all time. "Incoherent" implies the absence of this knowledge, which suggests the use of a statistical description.

II. STATEMENT OF THE PROBLEM

A single hydrophone monitors underwater acoustical energy for an observation time of T sec. If a signal is present, it is assumed to have the following form

$$s(t) = P \cos(\omega t + \varphi) \tag{1}$$

where P is assumed constant, the phase may or may not be known, and the frequency $\omega_i = 2\pi f_i$ is a random variable having a discrete probability density function

$$p(\omega) = \sum_{i=1}^{m} p(\omega_i)\, \delta(\omega - \omega_i) \tag{2}$$

where $\delta(x) = \begin{cases} 1 \text{ if } x = 0 \\ 0 \text{ if } x \neq 0 \end{cases}$ is the Kronecker delta function. That is, the signal appears at one of the frequencies ω_i, and is assumed to remain at that frequency for the duration of the observation interval. The frequency may possibly "wobble" slightly from interval to interval but is assumed to change so slowly that it is essentially constant for the period T.

The m possible frequencies at which the signal may appear are assumed to be contained in a low-frequency band of total width Ω.

The noise process received by the hydrophone, in addition to the signal (if present), is assumed to be a stationary, gaussian, random process with zero mean, and has a known spectral density N(f). The detector will be concerned with the values of f lying in $(-\Omega, \Omega)$, and thus N(f) is considered as being non-zero only in this band. The bandwidth is then Ω cps.

It is known from sampling theory that a waveform of duration T sec and bandwidth Ω cps may be approximately represented by a set of 2Ω T numbers. If the frequency band of the wave extends to zero cps, then these numbers are simply equally spaced amplitude samples of the wave. In the following, it will be mathematically convenient to treat the received waveform in terms of these 2Ω T amplitude samples. The actual detection system will not perform any sampling, however; the discrete representation is merely a technique to facilitate manipulation. The information thus presented to the detector is a vector $\underline{v}$ of n voltage samples where $n = 2\Omega T$. The column vector $\underline{v}$ has the transpose

$$\underline{v}' = [v(t_1), v(t_2), \ldots, v(t_n)] \tag{3}$$

$$v(t_i) = n(t_i) \quad \text{if signal is absent}$$

$$v(t_i) = n(t_i) + P \cos(\omega t_i + \varphi) \quad \text{if signal is present at frequency } \omega$$

It is well known that the optimum detector for a signal contaminated by a random noise is a likelihood ratio detector.[1] If any of the input quantities contain unknown parameters, the likelihood ratio must be averaged over all possible values of these quantities according to their probability distribution. For instance, if the signal contains the parameters θ_1 and θ_2 which are statistically independent but unknown a priori to the observer, the detector must form the averaged likelihood ratio

$$\Lambda(\underline{v}) = \int dP(\theta_1) \int dP(\theta_2)\, L(\underline{v}, \theta_1, \theta_2) \tag{4}$$

where the quantity $P(\theta_1)$ is the cumulative probability distribution function of θ_1, and similarly for $P(\theta_2)$. $L(\underline{v}, \theta_1, \theta_2)$ is the likelihood ratio, depending on the received vector $\underline{v}$, and assuming that the signal parameters have the particular values θ_1 and θ_2. The probability structure of the unknown parameters may or may not be known in a particular case. In the case where θ_1 is the phase angle of a sinusoidal signal, it is reasonable to assume that the angle φ is uniformly distributed in the interval 0, 2π. This assumption will be made in the following when the phase is assumed unknown.

Hence, in the two cases to be considered in this Memorandum: the coherent case where the phase angle is assumed known, and the incoherent case where it is assumed to be a uniformly distributed random variable, the two quantities must be formed

$$\text{Coherent} \qquad \ell(\underline{v}) = \sum_{i=1}^{m} L(\underline{v}, \omega_i)\, p(\omega_i) \tag{5}$$

$$\text{Incoherent} \qquad \ell(\underline{v}) = \sum_{i=1}^{m} p(\omega_i) \int_0^{2\pi} \frac{d\varphi}{2\pi} L(\underline{v}, \omega_i, \varphi) \tag{6}$$

The summation performs integration over the unknown but discretely distributed frequency parameter, according to Eq. (2). The two cases will be considered separately.

Although signal level is not known, it is not considered as a random variable here, and no averaging is performed over this parameter because the operations which the optimum detector performs are not

influenced by signal amplitude. The resulting detection performance depends very strongly on signal strength, but the detector can be built with no knowledge of how strong the signals will be.[1] Noise level, on the other hand, must be known in order to set a false-alarm rate.

III. DETECTION OF A SINE WAVE OF UNKNOWN FREQUENCY AND KNOWN PHASE

The case of detecting a single sine wave of known initial phase but unknown frequency has been considered in some detail by Levesque,[2] and this section reports his findings. It is realized that the assumption of known phase is unrealistic when the frequency is unknown, but it is believed that the following analysis is useful for two reasons: (1) it manipulates gaussian statistics and is therefore tractable, and (2) it places an upper bound on detectability which is later (Section IV) seen to be easily related to the unknown phase case results.

The optimum detector forms the quantity given in Eq. (5) and compares it with a preset threshold. If $\ell(\underline{v})$ exceeds this threshold, the decision is made that a signal is present. If $\ell(\underline{v})$ does not exceed the threshold, the signal is dismissed. Levesque introduces the concept of the decision hyperplane, which permits a geometrical interpretation of the decision process. Considering the simple case where the signal may appear at one of only two possible frequencies, m = 2, the averaged likelihood ratio takes the form

$$\ell(\underline{v}) = p(\omega_1)L_1 + p(\omega_2)L_2 \tag{7}$$

or

$$= p(\omega_1)\exp(\log L_1) + p(\omega_2)\exp(\log L_2) \tag{8}$$

where $L_1 = l(\underline{v}, \omega_1)$ and $L_2 = l(\underline{v}, \omega_2)$ for convenience. The form of Eq. (8) is used as it is usually more convenient to determine the quantity $\log L_i$ than the likelihood ratio itself. The optimum

detector compares the quantity of Eq. (8) with a threshold k, and a target-present decision is made depending on whether $\ell(\underline{v})$ exceeds this threshold or not. Thus, the "decision line" that separates one decision from the other is that which satisfies the equation

$$\ell(\underline{v}) = k \tag{9}$$

Assuming that the two possible frequencies are equally likely, $p(\omega_1) = p(\omega_2) = 1/2$, then Eqs. (8) and (9) yield

$$\log L_2 = \log[2k - \exp(\log L_1)] \tag{10}$$

as the equation of the "decision line." This line is shown in Fig. 1 for various values of the threshold k. As one of the quantities $\log L_1$ or $\log L_2$ becomes small, the decision curve rapidly approaches an asymptote parallel to one of the coordinate axes. In an actual system, a preset value of k is used, and thus one of the curves of Fig. 1 will form the boundary between the signal-accept and signal-dismiss regions. That is, the processed vector $\underline{v}$ yields the quantities $\log L_1$, $\log L_2$ which correspond to a point on the graph of Fig. 1. If this point lies above or to the right of the decision line given by Eq. (10), a signal-accept decision is made. If $\log L_1$ or $\log L_2$ lies below or to the left of this line, the signal-dismiss decision is made. If the number m of possible frequencies were greater than two, then the likelihood ratio of Eq. (5) would be compared to some other threshold. The resulting decision surface of m dimensions would divide an m-dimensional hyperspace into two regions: signal-accept and signal-dismiss. The processed data would yield m numbers,

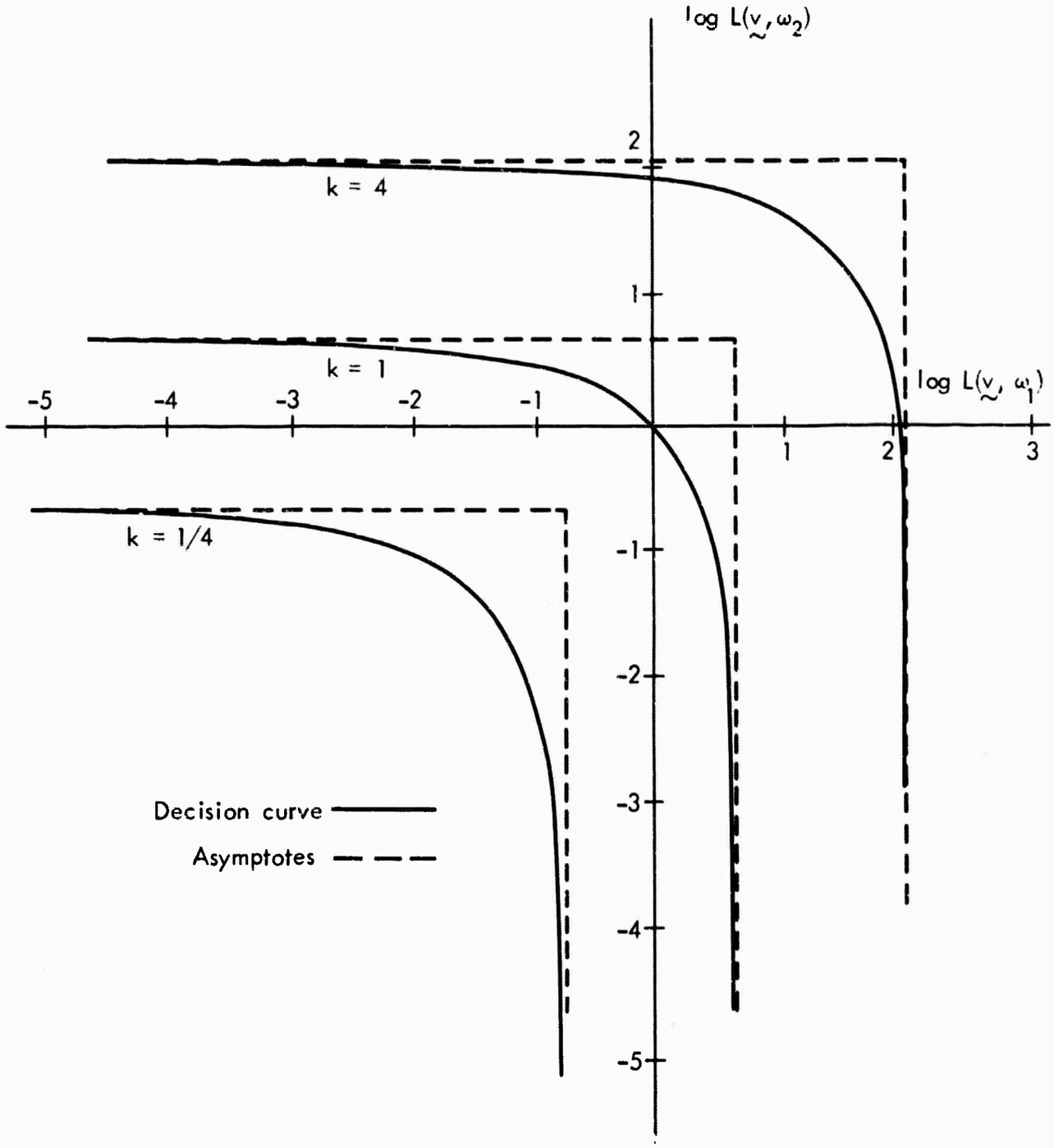

Fig. 1—Coherent sinusoid: decision curve for case of two possible frequencies (m = 2)

$\log L_1$, $\log L_2$, ..., $\log L_m$, corresponding to some point in the m-dimensional hyperspace; and the signal-accept decision is made if the point lies in the appropriate region. Otherwise, the signal-dismiss decision is made.

FORM OF THE LIKELIHOOD RATIO

The likelihood ratio $L(\underline{v}, \omega_i)$ may be written explicitly. It is well known that for a signal $s_i(t) = P \cos(\omega_i t + \varphi)$ imbedded in gaussian noise with covariance matrix $\underline{K}$, the likelihood ratio has the form

$$L(\underline{v}, \omega_i) = \exp\left[-\frac{1}{2} \underline{s}_i' \underline{K}^{-1} \underline{s}_i + \underline{s}_i' \underline{K}^{-1} \underline{v} \right] \tag{11}$$

Here $\underline{s}_i'$ is the row vector of time samples of the sinusoid at angular frequency ω_i. The noise covariance matrix $\underline{K}$ is related to the noise spectral density N(f) by the relation [Ref. 3, p. 103]

$$R(\tau) = \int_{-\infty}^{\infty} N(f) \exp(j\omega\tau)\, df \tag{12}$$

$$\underline{K} = \begin{bmatrix} P_o & R_1 & \cdots & R_{n-1} \\ R_1 & R_o & \cdots & R_{n-2} \\ \cdot & & & \cdot \\ \cdot & & & \cdot \\ \cdot & & & \cdot \\ R_{n-1} & \cdots & & R_o \end{bmatrix}$$

where $R_i = R\left(\frac{i}{2\Omega}\right)$ and $\frac{1}{2\Omega}$ = time between samples.

The logarithm of the likelihood ratio of Eq. (11) has the form

$$\log L_i = -\frac{1}{2}\,\underline{s}_i'\,\underline{K}^{-1}\,\underline{s}_i + \underline{s}_i'\,\underline{K}^{-1}\,\underline{v} \tag{13}$$

The second term indicates that the detector must correlate the received waveform with the signal at the i^{th} frequency. For example, if the noise is assumed to have a flat spectral density of level $N_o/2$ volts^2/cps over the band of all possible frequencies $(-\Omega, \Omega)$, then the matrix $\underline{K}$ is given by $N_o\underline{I}\,\Omega$, where $\underline{I}$ is the unit matrix, the noise variance $N = N_o\Omega$, and the correlation portion of Eq. (13) becomes

$$\underline{s}_i'\,\underline{K}^{-1}\,\underline{v} = \frac{1}{N_o\Omega}\sum_{j=1}^{n} P\cos(\omega_i t_j + \varphi)\,v(t_j) \tag{14}$$

$$\doteq \frac{2P}{N_o}\int_o^T v(t)\cos(\omega_i t + \varphi)\,dt \tag{15}$$

Equation (15) approximates the sum of Eq. (14) by an integral and makes use of the relation $dt \doteq \Delta t \doteq 1/(2\Omega)$.

The first part of Eq. (13) may likewise be analyzed, and it is seen to become

$$-\frac{1}{2}\,\underline{s}_i'\,\underline{K}^{-1}\,\underline{s}_i \doteq -\frac{1}{2}\,\frac{1}{N_o\Omega}\sum_{j=1}^{n} P^2\cos^2(\omega_i t_j + \varphi) \tag{16}$$

$$\doteq -\frac{1}{2}\,\frac{2}{N_o}\int_o^T P^2\cos^2(\omega_i t + \varphi)\,dt$$

$$\doteq -\frac{1}{2}\,\frac{P^2T}{N_o} \tag{17}$$

as long as T is large in comparison to each sine wave period, $\frac{2\pi}{\omega_i}$. It is convenient to define the "detection index," d, which satisfies

$$d^2 = P^2T/N_o \tag{18}$$

Thus, d^2 is the signal-to-noise ratio at the output of the detector at the end of the observation period of T sec and may be used as a figure of merit in evaluating detectability. This is not the signal-to-noise power ratio at the input to the detector, which has the value $P^2/2N$, but it is the ratio after the detector has processed the received data. By comparing input and output signal-to-noise ratios, it is seen that the "processing gain" is $2\Omega T$, the number of degrees of freedom in the sampling representation. Note that although P and therefore d are not known a priori, they can be used here as if they were known, and the results can be presented in terms of d as a parameter.

PERFORMANCE OF THE DETECTOR

It remains to calculate the performance of the detector. This requires finding the probabilities of false alarm and detection for

particular settings of the threshold and for particular values of input signal-to-noise ratio. In order to do this, the conditional joint distributions of the test quantities $\log L_1$, $\log L_2$ must be computed under the three hypotheses

$$H_o: \text{ no signal present, } v(t) = n(t) \tag{19}$$

$$H_1: \text{ signal present at } \omega_1, \; v(t) = n(t) + s_1(t) \tag{20-a}$$

$$H_2: \text{ signal present at } \omega_2, \; v(t) = n(t) + s_2(t) \tag{20-b}$$

Levesque has done this, and the derivations appear in Appendix A. It is shown there that the resultant joint distribution is gaussian and that the quantities $\log L_1$ and $\log L_2$ are approximately independent since there is almost no correlation between sine waves of different frequencies over a long observation time, a time such that $\Omega T >> 1$ and $|\omega_1 - \omega_2| T >> 1$. This is exactly true if $|\omega_1 - \omega_2|$ is a multiple of $2\pi/T$ cps. The results are

$$f(x_1,x_2/H_o) = \frac{1}{2\pi d^2} \exp\left[- \frac{\left(x_1 + \frac{d^2}{2}\right)^2 + \left(x_2 + \frac{d^2}{2}\right)^2}{2d^2} \right] \tag{21}$$

$$f(x_1,x_2/H_1) = \frac{1}{2\pi d^2} \exp\left[- \frac{\left(x_1 - \frac{d^2}{2}\right)^2 + \left(x_2 + \frac{d^2}{2}\right)^2}{2d^2} \right] \tag{22}$$

$$f(x_1,x_2/H_2) = \frac{1}{2\pi d^2} \exp\left[- \frac{\left(x_1 + \frac{d^2}{2}\right)^2 + \left(x_2 - \frac{d^2}{2}\right)^2}{2d^2} \right] \tag{23}$$

where for convenience $x_i = \log L_i$; $i = 1, 2$.

It is noted that the shift in the mean value of, say, x_1, between the cases of signal absent and signal present, is equal to d^2. The standard deviation of x_i is d. Thus, the ratio of the shift in the mean over the standard deviation is given by d itself. The square of such a ratio is frequently used as the output signal-to-noise ratio in detection problems. This reinforces the choice of d or d^2 as a figure of merit.

Using these probability density functions, it is convenient to use the geometrical approach of the decision space to calculate the performance probabilities. These three functions are represented in Fig. 2, where the contours of constant probability are centered around the mean values of the density functions. For the value of threshold shown, it is seen that under the hypothesis H_o noise only is present, and there is some probability that the point $\log L_1$, $\log L_2 = x_1, x_2$ will actually fall above the threshold decision curve. This false-alarm probability may be found by integrating the density function of Eq. (21) over the entire region above and to the right of the decision curve. Using Eq. (10) of the decision curve, this gives

$$\alpha = \int_{\log 2k}^{\infty} dx_2 \frac{1}{\sqrt{2\pi}\, d} \exp\left[- \frac{1}{2d^2} \left(x_2 + \frac{d^2}{2} \right)^2 \right] +$$

$$\int_{-\infty}^{\log 2k} dx_2 \frac{1}{\sqrt{2\pi}\, d} \exp\left[- \frac{1}{2d^2} \left(x_2 + \frac{d^2}{2} \right)^2 \right] \cdot \qquad (24)$$

$$\int_{\log_e 2k - \exp(x_2)}^{\infty} dx_1 \frac{1}{\sqrt{2\pi}\, d} \exp\left[- \frac{1}{2d^2} \left(x_1 + \frac{d^2}{2} \right)^2 \right]$$

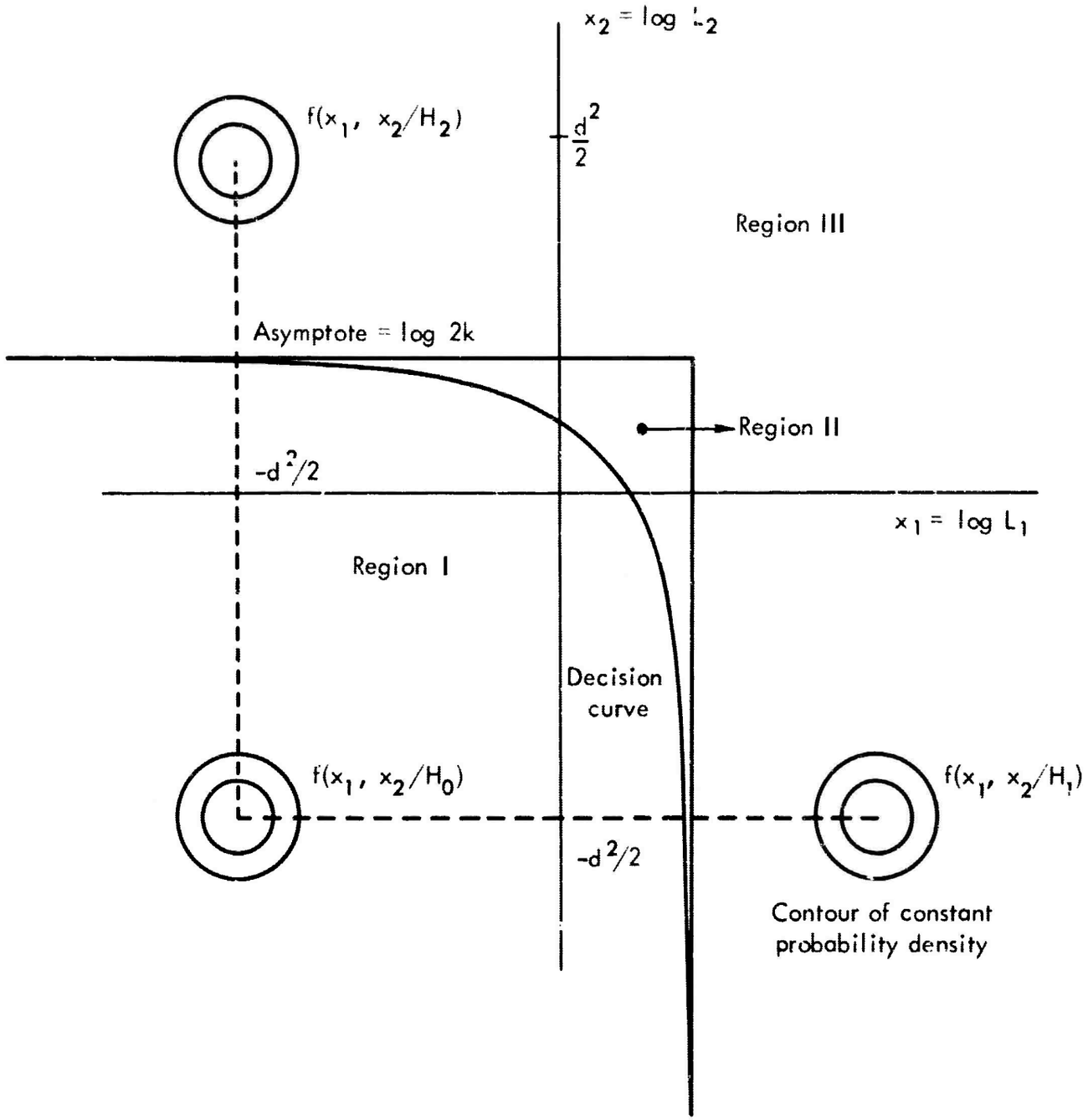

Fig. 2—Location of probability density functions relative to decision regions under three hypotheses for m = 2 case

Unfortunately, the lower limit determined by the decision curve in the above integral renders the integral unsolvable in closed form. A useful approximation to the value of the integral may be made by using the asymptote to the decisic curve instead of the exact curve itself. To understand the effect of this approximation, consider the following argument.

It is seen from Fig. 2 that the probability density funccions of x_1, x_2 are centered about the values $\pm d^2/2$. Thus, as the signal-to-noise ratio increases, the centers of these distributions move away from the origin and move further away from the decision line. If the distributions are far from this line, its exact shape is no longer important, and the asymptotes may be used. Another way of considering this is to examine the area, Region II, involved in the approximation. By using the asymptotes, Region II is effectively added to the "signal absent" decision portion, when it really belongs to the "signal present" decision portion. The error then is equal to the probability density integrated over Region II. But, as the distributions move further away with increasing d^2, their value within this area decreases rapidly. Therefore, it may be said in general that for large output signal-to-noise ratios, the asymptotes may give a very good approximation. Since the asymptotes are parallel to the coordinate axes in both this and the $m > 2$ cases, the use of the asymptotes for the decision curve is analogous to making a decision based on each quantity for $\log L_1$ independently. Levesque calls this behavior the "band-splitting" detector, since it treats the processed received signal at each of the m different frequencies independently.

The detector approaches a maximum-likelihood detector for large output signal-to-noise ratios. Again, it should be pointed out that the signal-to-noise ratio in question is that at the output after processing. For small input signal-to-noise ratios, the output signal-to-noise ratio may be increased many times by a long integration time, as indicated by Eq. (18). Since only in the case of fairly large output signal-to-noise ratios is there any chance of detection, these are the primary cases of interest. Hence, this approximation will be used in the following.

Returning to the evaluation of the false-alarm probability, α, and using the value of the asymptote in the lower limit of the integration of Eq. (24), $\log[2k - \exp(x_2)] \doteq \log(2k)$, α may be evaluated. With a change of variable, Eq. (24) becomes

$$\alpha \doteq \frac{1}{\sqrt{2\pi}} \int_a^\infty \exp\left(\frac{-v^2}{2}\right) dv \tag{25}$$

$$+ \frac{1}{2\pi} \int_{-\infty}^{a} \exp\left(\frac{-v^2}{2}\right) dv \int_a^\infty \exp\left(\frac{-u^2}{2}\right) du$$

$$= \frac{1}{4}\left[1 - \Phi(a)\right]\left[3 + \Phi(a)\right] \tag{26}$$

where

$$a = \frac{d}{2} + \frac{1}{d} \log 2k \tag{27}$$

and where $\Phi(x) = \frac{1}{\sqrt{2\pi}} \int_{-x}^{x} e^{\frac{-t^2}{2}} dt$ is the normal probability integral

given in tables.[4] Using this result, the proper threshold may be set for an allowable false-alarm probability per observation time.

The probability of detection is the probability that the values $\log L_1$, $\log L_2$ will lie above the threshold curve under either of the hypotheses H_1, H_2 (for equally likely signals). This is more conveniently found by computing the miss probability, β, which is equal to one minus the detection probability $\beta = 1 - P_d$, the probability that the test quantities yield a point that lies below the threshold, even though a signal is actually present. Again, using the asymptotic approximation and the same nomenclature

$$\beta = 1 - P_d \doteq \frac{1}{2\pi} \int_{-\infty}^{a-d} e^{\frac{-v^2}{2}}\, dv \int_{-\infty}^{a} e^{\frac{-u^2}{2}}\, du \tag{28}$$

$$= \frac{1}{4}\left[1 - \Phi(d - a)\right]\left[1 + \Phi(a)\right] \tag{29}$$

Curves of P_d versus d are given in Fig. 3 for various values of false-alarm probability. As discussed later in this section, these curves must be straight lines on normal probability scales. The dotted curves are shown for values of detection probability less than 50 percent, to indicate that the asymptotic decision curve approximation begins to break down. Actually, an error check was made for $\alpha = .01$ and $P_d = 50$ percent, which requires $d = 2.6$, with the result that the probability of the vector (x_1, x_2) falling in the error region, Region II, is 1.506 percent. Therefore, the correct curve of P_d versus d would curve up slightly as d decreases and at $d = 2.6$ would show $P_d = 51.506$ percent. For higher values of detection

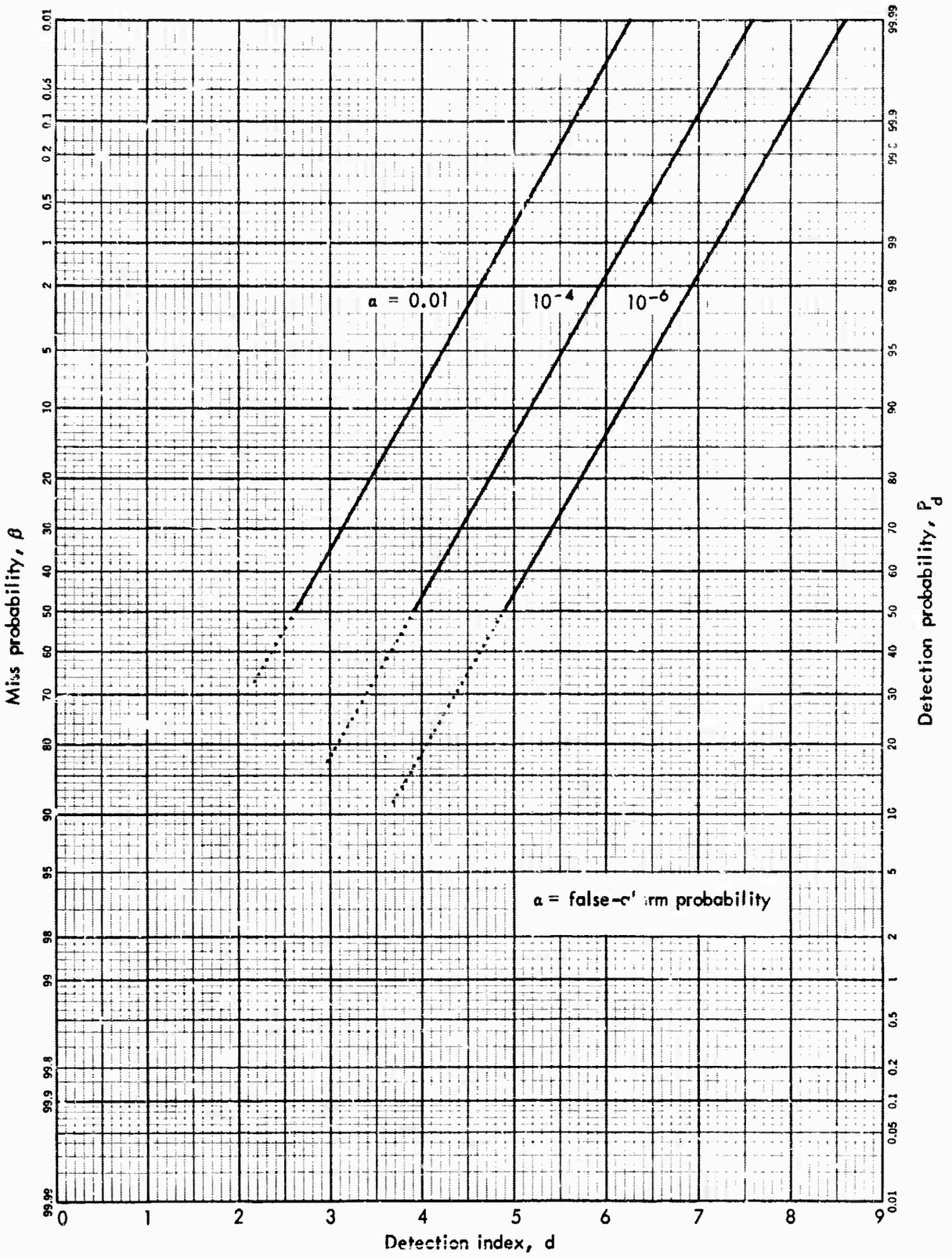

Fig. 3—Coherent sinusoid: signal detectability for case of two possible frequencies (m = 2)

probability and/or lower values of false-alarm probability, this error would de . very rapidly.

It must be stressed again that this is only an error in the analytical results to facilitate a closed-form solution. It does not reflect an error made by the system. For the example given above, the actual system has a detection probability 1.5 percent higher than that shown in Fig. 3. A negligible error is made in the calculation of α, since the density function as seen in Fig. 2 is situated so far from Region II.

m-FREQUENCY CASE

If the number of possible frequencies at which the signal might appear is greater than 2, the decision surface is now m-dimensional and satisfies, according to Eq. (5), for equally probable frequencies ω_i

$$\sum_{i=1}^{m} \exp[\log L_i] = mk \tag{30}$$

where k is the preset threshold, and $\log L_i$ is the quantity described by Eq. (11) for each frequency ω_i. In order to calculate the performance probabilities, it is necessary to find the joint conditional probability distributions of the m test quantities $\log L_i$, $i = 1, 2, \ldots, m$, under each of the hypotheses H_o, H_1, H_2, ..., H_m, where H_i indicates the assumption that a signal is present at the i^{th} frequency ω_i. It is clear from the analysis of Appendix A that the result will be an m-dimensional normal distribution of uncorrelated variables, and

1. if no signal is present, all of the m quantities $\log L_i$, $i = 1, 2, \ldots, m$ will have mean values $-d^2/2$;

2. if a signal is present at ω_j, m - 1 of the quantities will have negative mean values of $-d^2/2$, and the quantity log L_j will have a positive mean value of $d^2/2$.

The m-dimensional normal distributions must be integrated over a portion of the decision space determined by the decision surface of Eq. (30). Although the actual detector will form the sum of Eq. (30) and compare this sum with the threshold, for purposes of analysis it is necessary to make the approximation to the asymptotic decision surface as was done in the m = 2 case. If d^2 is large (due, for instance, to a long observation time), then the mean values of the quantities mentioned above will be large, either negative or positive. In Eq. (30) it is seen that if one term is larger than the others, as will be the case when a signal is present at one of the ω_i, the exponentiation performed will markedly accentuate this term and also depress the other terms. Thus, the detector will be effectively making its decision based on only one term. This is equivalent to a maximum likelihood detector for which the asymptotic decision curves are appropriate.

The error probabilities may easily be computed by combinatorial methods. Since the m quantities log L_i, i = 1, 2, ..., m are statistically independent, and for large d^2 the asymptotic decision curve approximation is made so that a decision results according to each value log L_i alone, an overall false alarm will result if any one of the quantities log L_i causes a false alarm. Each test quantity is normally distributed with variance d^2, and with mean

values $-d^2/2$ or $+d^2/2$ under hypotheses H_o and H_i respectively. Here it is understood that H_o indicates the hypothesis that no signal is present in the i^{th} quantity, although it may be present at some other frequency. Thus, for each test quantity, the false-alarm and false-dismissal probabilities (α_i and β_i respectively) are given by

$$\left\{ \begin{matrix} \alpha_i \\ \beta_i \end{matrix} \right\} = \frac{1}{2}\left[1 - \Phi\left(\frac{d}{2} \pm \frac{1}{d} \log mk\right)\right] \tag{31}$$

where the asymptotic threshold value log mk is used. The detector rings a false alarm if any one of the m quantities causes a false alarm. The probability of this event is given by

$$\alpha = 1 - (1 - \alpha_i)^m \approx m\alpha_i \tag{32}$$

for small $m\alpha_i << 1$. In addition, a false dismissal occurs when all of the m quantities do not exceed the threshold, under the condition that there is a signal present at one of the frequencies. Since the m test quantities are identically distributed, it makes no difference at which one the signal actually appears, that is, which of the quantities log L_i produces the false dismissal. Hence, a false dismissal occurs whenever there are m - 1 correct dismissals and one false dismissal, and has a probability of occurring

$$\beta = \beta_i(1 - \alpha_i)^{m-1} \approx \beta_i \tag{33}$$

again for $m\alpha_i << 1$.

The probability of detection, $P_d = 1 - \beta$, is plotted in Fig. 4 for several values of m and for false-alarm probabilities of 10^{-2} and 10^{-6}. It is seen that detectability decreases as m increases, which is reasonable since there is greater chance of an error with a large number of independent processors. Also, using the approximations of Eqs. (32) and (33), Eq. (31) may be used to solve for log mk in terms of the allowable false-alarm probability α^*. Using this value of threshold to compute false-dismissal probability by Eq. (31)

$$1 - \beta \doteq \frac{1}{2}\left\{1 + \Phi\left[d - \Phi^{-1}\left(1 - \frac{2\alpha^*}{m}\right)\right]\right\} \tag{34}$$

for large values of d^2 where $\Phi^{-1}(\cdot)$ is the inverse function to $\Phi(\cdot)$. It is thus seen that $P_d = 1 - \beta$ is a linear function of d on normal probability scales, since the argument of the inverse normal probability function is constant with respect to d. This sheds light on the linearity of the detection probability curves versus d, for constant α. Finally, it should be noted that the loss in detectability resulting from doubling the number of possible frequencies m in which the signal may appear is equivalent to subtracting about .15 from the detection index at very low values of α, and a slightly greater amount at larger values of α. The curve for m = 1 is the known frequency and known phase detection case.

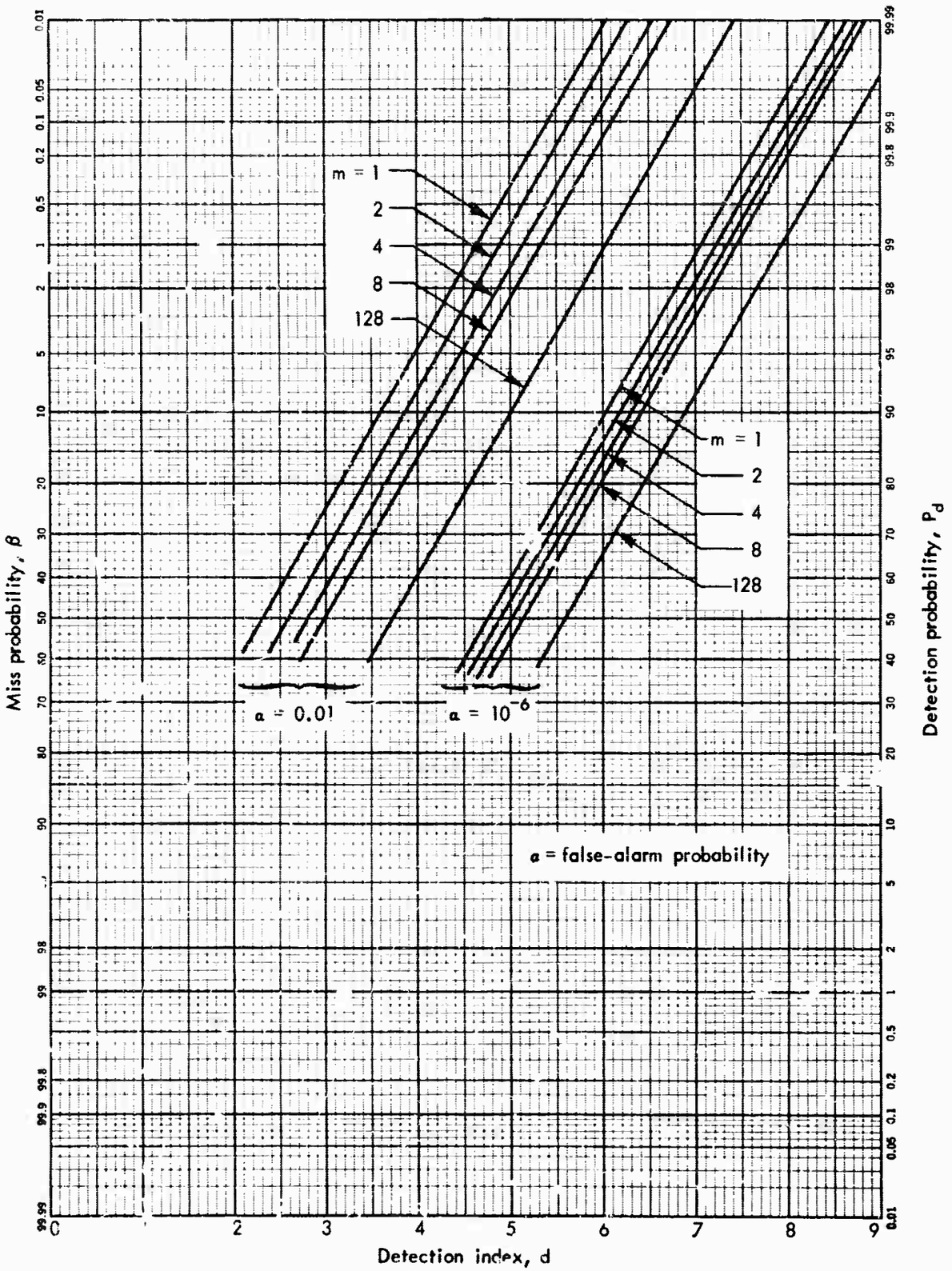

Fig. 4—Coherent sinusoid: signal detectability for case of m possible frequencies

IV. DETECTION OF AN INCOHERENT SINUSOID OF UNKNOWN FREQUENCY

The more realistic case of the detection of a sine wave of both unknown frequency and phase is now considered. The signal again has the form described in Eq. (1), but now the phase φ is also random and uniformly distributed in $(0, 2\pi)$. The resulting likelihood ratio, which performs the average over both frequency and phase, is given in Eq. (6). The quantity in the summand has been treated extensively in the literature,[1,3] as it is the likelihood ratio for a sine wave of known frequency and constant amplitude but unknown phase. For white gaussian noise, the summand becomes

$$\frac{1}{2\pi} \int_0^{2\pi} d\varphi \, L(\underline{v}, \omega_i \varphi) = C \, I_o(r_i) \tag{35}$$

where C is a constant proportional to the output signal-to-noise power ratio, $I_o(x)$ is the zero-order modified Bessel function,[4] and the quantity r_i is given by

$$r_i = \frac{2P}{N_o} \sqrt{\left\{ \int_o^T v(t) \cos \omega_i t \, dt \right\}^2 + \left\{ \int_o^T v(t) \sin \omega_i t \, dt \right\}^2} \tag{36}$$

Each test quantity r_i is formed by cross-correlating the received signal v(t) with the two quadrature-component sinusoids at the i^{th} frequency. If a signal at ω_i is indeed present in v(t), it cannot simultaneously be out of phase with both of the quadrature-component sinusoids; consequently, at least one of the cross-

correlations must yield a non-zero value. r_i then forms the normalized rms value of these two cross-correlations. The quantity r_i may also be generated by passing v(t) through a filter with impulse response

$$h_{opt}(t) = \begin{cases} K \cos \omega_i (T - t) & 0 \le t \le T \\ 0 & t > T \end{cases} \tag{37}$$

for some constant K followed by an amplifier with a gain of $2P/N_o K$. This may be seen since the output of the filter at time T is given by the convolution integral as

$$v_o(T) = \frac{2P}{N_o} \int_o^T v(\tau) \cos \omega_i \tau \, d\tau \tag{38}$$

The final likelihood ratio which the detector must form becomes, for equally likely frequencies

$$\ell(\underline{v}) = \frac{1}{m} C \sum_{i=1}^{m} I_o(r_i) \tag{39}$$

The optimum detector consists of a bank of narrow-band filters, each centered at one of the m possible frequencies which the signal might have. Thus, the optimum detector forms m terms r_i, i = 1, ..., m according to Eq. (36), and passes each r_i through a nonlinear device that takes its modified Bessel function. These quantities are then summed, and the result is compared to a threshold. This is shown schematically in Fig. 5 on the following page, where, for simplicity, the term $\frac{C}{m}$ has been removed from $\ell(\underline{v})$ above and used to modify a threshold c. The final threshold is called k. This threshold will be adjusted to fix the false-alarm probability at the allowable maximum, and so its exact form here is not important.

By performing the analysis first for the simple m = 2 case, the likelihood ratio of Eq. (39) becomes, with the constant term removed

$$\ell = I_o(r_1) + I_o(r_2) \tag{40}$$

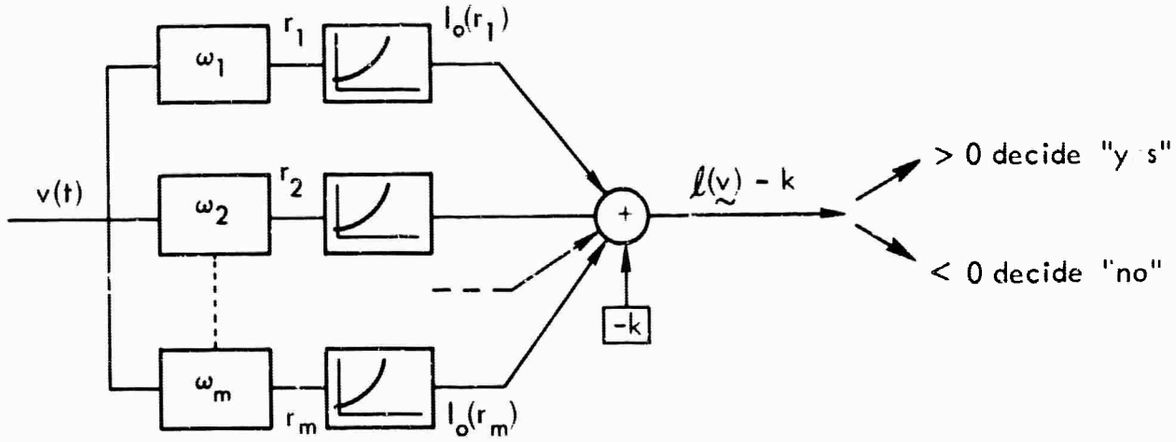

Fig. 5—Form of optimum detector

The detector forms this quantity and compares it with the threshold k. If the sum exceeds k, the signal-accept decision is made. If the sum does not exceed k, the signal-dismiss decision is made. A decision curve may be formed in direct analogy to the coherent detector case, and for m = 2, it will satisfy

$$I_o(r_1) + I_o(r_2) = k \tag{41}$$

Using the coordinates r_1, r_2, this curve is plotted in Fig. 6 for various values of k, along with the asymptotic values

$$r_1, r_2 = I_o^{-1}(k - 1) \tag{42}$$

where $I_o^{-1}(\cdot)$ is the inverse modified Bessel function. The use of the term asymptote is retained here by analogy with the coherent case, even though there is strictly no asymptotic value since r_1 and r_2

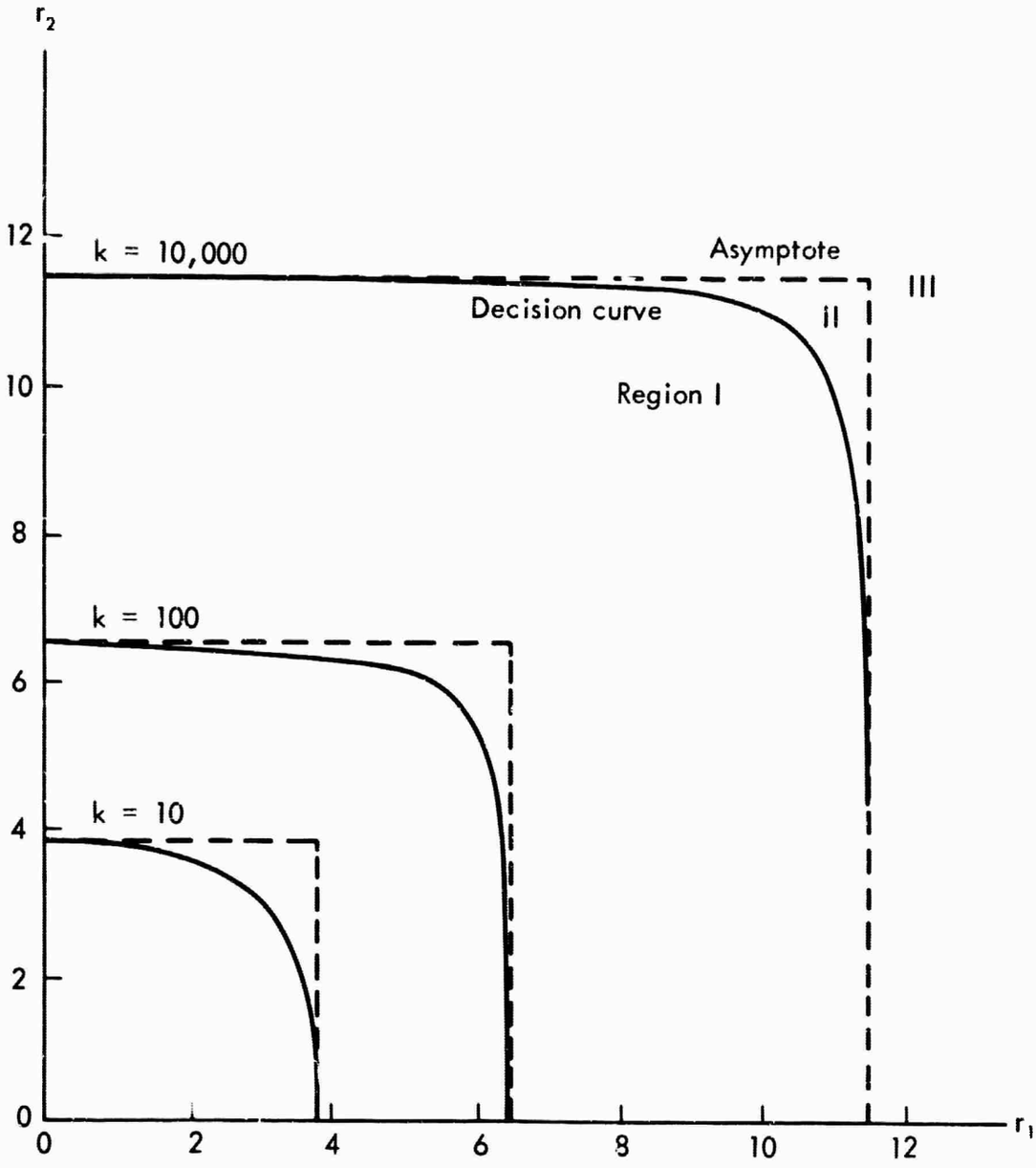

Fig.6—Incoherent sinusoid: decisior curve for case of two possible frequencies (m = 2)

are always non-negative. By the asymptotic values here is meant the largest value of r under the decision curve, or the value of the decision curve when one envelope is zero (note, $I_o(0) = 1$). It is seen in Fig. 6 that the decision curve does not approach its asymptote as quickly as in the last case, shown in Fig. 1. However, the area of Region II is approximately constant for different values of k, and thus for large signal-to-noise ratios this area becomes proportionately less important. For example, later calculations will show that the threshold value k changes very rapidly with signal-to-noise ratio and false-alarm probability. As d^2 (later shown to be the signal-to-noise ratio) increases, or α decreases, the necessary value of k increases exponentially. To use two examples, for a detection probability of 70 percent with a false-alarm probability of .01, the required value of d is 3.65, and $k \doteq 17{,}000$. For a detection probability of 90 percent with a false alarm of .0001, the required d is 5.6, and $k \doteq 5 \times 10^8$. For such large values of k, the error in using the asymptote is clearly negligible.

In conjunction with the examples above, it should be remembered that the false-alarm probability α occurs in each observation interval. If it is desired to calculate from this probability the expected number of false alarms per year, α is simply multiplied by the number of observation intervals in one year. This is so because the occurrence of false alarms is independent from one interval to the next, and therefore the number of false alarms in one year is binomially distributed with mean value $q\alpha$, where q is the number of observation intervals in one year. For example, if $\alpha = .0001$ and

each interval lasts 5 min, there are approximately 100,000 intervals per year, and the expected number of false alarms per year is 10.

PERFORMANCE OF THE DETECTOR

In order to find the probabilities of false alarm and detection, the joint distribution of the test quantities r_i, $i = 1, 2, \ldots, m$ must again be found under the various hypotheses H_o, H_1, ..., H_m as defined earlier. Due to the fact that the correlators of Eq. (36) process the received waveform for only a time T, they exhibit an effective bandwidth of approximately 2/T cps. More precisely, each correlator, or filter and amplifier, given by Eq. (37), has the effective frequency response characteristic [Ref. 5, p. 314]

$$|H_i(f)| = \frac{PT}{N_o} \frac{\sin\left(2\pi|f - f_i|\frac{T}{2}\right)}{2\pi|f - f_i|\frac{T}{2}} \qquad (f > 0) \tag{43}$$

The mirror image of this response is, of course, also present at negative frequencies. Thus, if two possible signal frequencies lie near each other, there will be some overlap in their correlator responses, as shown in Fig. 7. It is seen, however, that this overlap

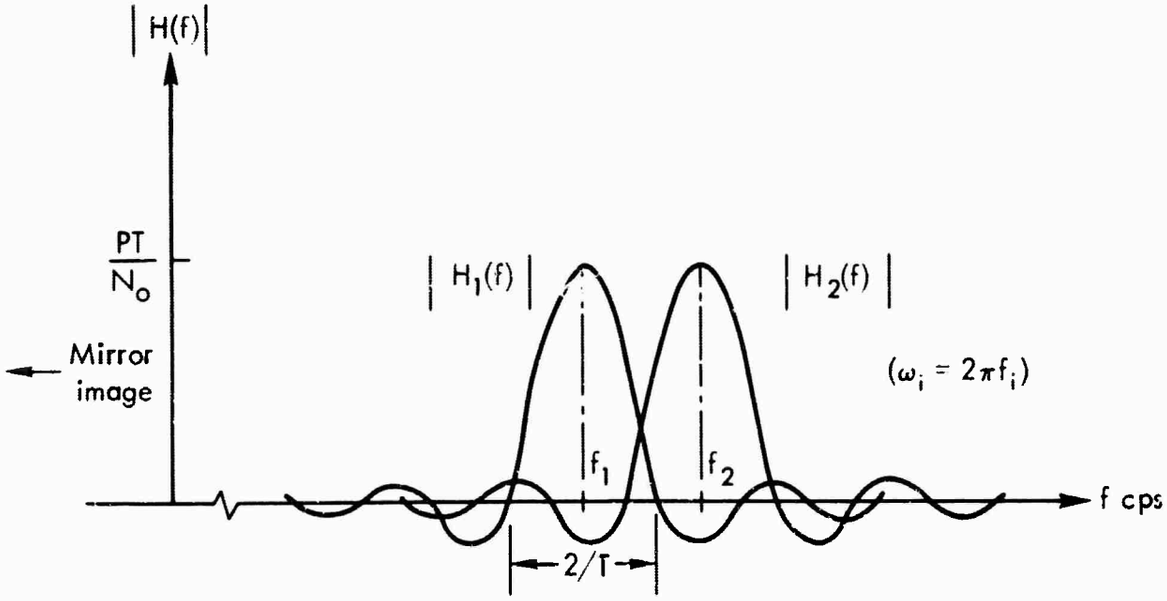

Fig. 7—Effective characteristics of filters

is small if f_1 and f_2 differ by more than 2/T cps. When T is large, therefore, there should be very little dependence between the output signals from such correlators. This is shown more precisely in Appendix B, where the joint probability density function of the outputs r_1 and r_2 is calculated. It may be seen there, for example, that the correlation between r_1 and r_2 is given very closely by

$$\psi_{12} \doteq d^2 \frac{\sin(\omega_2 - \omega_1)\frac{T}{2}}{(\omega_2 - \omega_1)\frac{T}{2}} \tag{44}$$

if ω_2 is close to ω_1, the case of interest, and is very nearly equal to

$$\psi_{12} \doteq 2d^2 \frac{\sin \omega_2 \frac{T}{2}}{\omega_2 \frac{T}{2}} \qquad \text{(if, say, } \omega_2 >> \omega_1\text{)} \tag{45}$$

if ω_2 and ω_1 are widely separated. The quantity ψ_{12} is a measure of the dependence given by Eq. (B-21), and depends on the cross moments defined in Eqs. (B-8) and (B-10). It can be seen that two conditions will insure that this dependence is negligible: $|\omega_2 - \omega_1| T >> 1$, and for each frequency ω_i $T >> 1$. This will always be true in practice. Thus, the envelopes are independent, and their joint distribution under each hypothesis can be obtained from Appendix B. For noise only

$$p(r_1, r_2/H_o) = \frac{r_1 r_2}{d^4} \exp\left[-\frac{1}{2d^2}(r_1^2 + r_2^2)\right] \tag{46}$$

and for signal plus noise

$$p(r_1, r_2/H_2) = \frac{r_1 r_2}{d^4} \exp\left[-\frac{1}{2d^2}(r_1^2 + r_2^2 + d^4)\right] I_o(r_2) \tag{47}$$

where the signal-to-noise ratio, or detection index d^2, is identical to that of the coherent case

$$d^2 = P^2 \frac{T}{N_o} \tag{48}$$

Under hypothesis H_1 that the signal appears instead at ω_1, the subscripts in Eq. (47) need only be reversed.

ACTUAL FILTER PERFORMANCE

Having obtained a set of correlators as the desired results for the optimum detector, it is instructive at this point to digress to the subject of real narrow-band filters in order to compare their performance with that of the optimum detector above. It was seen that the effective bandwidth of the correlator acting for time T was approximately 2/T cps. This is the minimum attainable bandwidth for any actual filter acting only for T sec, as is well known from the uncertainty principle [Ref. 1, p. 21]. Thus, if an actual RLC filter having a bandwidth much narrower than 2/T were used, the filter would be expected to approximate very closely the optimum detector. The RLC filter is considered to have impulse response equal to

$$h(\tau) = K_1 e^{-\epsilon\tau} \cos(\omega_i \tau + \varphi) \tag{49}$$

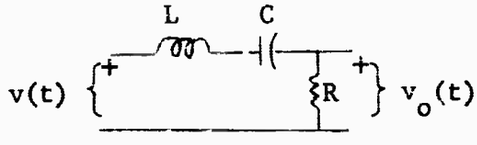

where $\epsilon = R/2L$, $\omega_i^2 = \omega_o^2 - \epsilon^2$, $\omega_o^2 = 1/LC$, $\tan \varphi = \epsilon/\omega_i$, and $K_1 = 2\epsilon\omega_o/\omega_i$. This is followed by an amplifier having a gain of $2P/N_c K_1$, in order to conform with Eq. (38). The bandwidth of the filter defined by the half-power frequencies is 2ϵ cps. At time T, the output voltage is given by

$$v_o(T) = \frac{2P}{N_o} \int_o^T v(\tau)\, e^{-\epsilon(T-\tau)} \cos[\omega_i(T - \tau) + \varphi]\, d\tau \qquad (50)$$

It is shown in Appendix C that for an input noise process v(t) with spectral density of level $N_o/2$ volts^2/cps over a band $(-\Omega, \Omega)$ that is wide with respect to the passband of the filter, the variance of the output process (at time T) is given by

$$\psi_{fil} = \frac{P^2 T}{N_o} \qquad (\epsilon T << 1) \qquad (51)$$

The autocorrelation function for such a process when the filter has impulse response existing only for time T is also given there. In order to find the signal-to-noise ratio at the output, it is necessary to find the effect of the filter on an input sine wave. As shown in Appendix B, the signal-to-noise ratio d^2 is equal to the square of the envelope output due to a sine wave alone at time T, divided by the output variance due to the noise input. (Due to the non-gaussian statistics, this is somewhat different from the coherent case, where d^2 was simply the square of the shift in the mean value of the output from the noise only to the signal plus noise cases, divided by the output variance.) The envelope output may be found as shown in Appendix C. This value is

$$r(T) = \frac{P^2 T}{N_o} \qquad (\epsilon T << 1) \qquad (52)$$

It is clear that when this is squared and divided by the value in Eq. (51), the same value is obtained for the signal-to-noise ratio, d^2, as before, demonstrating that the filter performs as well as the optimum detector as long as $\epsilon T << 1$.

Consider now the case when this is not true. In practice, with observation times in the order of hundreds of seconds, it is very difficult to build filters with bands narrow enough to satisfy this condition. Practicable filters will have too wide a bandwidth, which will admit too much noise power, thus degrading the resulting signal-to-noise ratio. This is shown in detail in Appendix C, where using the above filter, it is seen that the variance of the noise output at time T (provided that $\omega_i T >> 1$) is

$$\psi_{fil} = \frac{P^2}{2\epsilon N_o}\left[1 - e^{-2\epsilon T}\right] \tag{53}$$

when ϵT is no longer much less than unity. This is seen to approach the previous value as ϵT diminishes. Also, the envelope output at time T for a sine wave alone is shown to be

$$r(T) = \frac{P^2}{\epsilon N_o}\left[1 - e^{-\epsilon T}\right] \tag{54}$$

Squaring this and dividing as before by the variance in Eq. (53), the signal-to-noise ratio, or detection index, d^2_{fil}, for the filter detector when the filter has a bandwidth no longer narrow enough (ϵT is no longer necessarily much less than unity) is

$$d^2_{fil} = \frac{P^2 T}{N_o} \cdot \frac{2}{\epsilon T} \cdot \frac{1 - e^{-\epsilon T}}{1 + e^{-\epsilon T}} \tag{55}$$

It is thus seen that a degradation factor is introduced, the ratio of the signal-to-noise ratios for the optimum and the filter detectors. This factor has the value

$$D^2 = \frac{2}{\epsilon T} \cdot \frac{1 - e^{-\epsilon T}}{1 + e^{-\epsilon T}} \tag{56}$$

and it seen to approach unity as ϵT approaches zero, and it approaches zero as ϵT becomes large.

The above result for d_{fil}^2 may be used directly in Eqs. (46) and (47), as long as the filter outputs are approximately independent. It can be seen from the derivation in Appendix B that the dependence between the envelopes is given by the quantity $\psi_{12}^2 = \mu_{13}^2 + \mu_{14}^2$, where the latter quantities are cross moments between the quadrature components of the two filters. Using the technique shown there, and assuming that two identical filters are used, of the form of Eq. (49), it is a straightforward although tedious matter to show that the normalized dependence $\rho^2 = \psi_{12}^2/\psi_{fil}^2$ is given by

$$\rho^2 = \frac{4\epsilon^2}{4\epsilon^2 + (\omega_2 - \omega_1)^2} \frac{e^{-4\epsilon T} - 2e^{-2\epsilon T}\cos(\omega_2 - \omega_1)\,T + 1}{1 - e^{-2\epsilon T}} \qquad (57)$$

which is small whenever $2\epsilon << |\omega_2 - \omega_1|$; that is, whenever the filter bandwidth is much smaller than the spacing between the filter center frequencies (possible signal frequencies). This assures approximate independence between r_1 and r_2, and Eq. (55) can be used to calculate the signal-to-noise ratio when real RLC filters are used in place of the optimum correlators. This in turn may be used to calculate the performance probabilities of the detector, according to the relations given below.

PERFORMANCE PROBABILITIES

Using the decision curve discussed previously, the probabilities of false alarm and detection may now be calculated. For large values of signal-to-noise ratio at the output of the detector, the asymptotic approximation to the optimum decision curve may be used, as the type

of argument made in connection with the coherent detector decision space applies here as well. That is, for large output signal-to-noise ratios, Region II of Fig. 6 has little significance since the centers of the distributions in question, those of Eqs. (46) and (47), are located far from this region. In particular, if there is no signal present in the i^{th} filter, the output has a mean value $r_i = d$. If there is a signal present in this filter, the output has a mean value $r_i = d^2$. The mean values are separated by the factor d.

In the actual calculation, the false-alarm probability α is easily computed by noting that $1 - \alpha$ is the probability that the point r_1, r_2 lies below the threshold, given H_o

$$\alpha = 1 - \int_o^b dr_1 \int_o^b dr_2 \frac{r_1 r_2}{d^4} \exp\left[- \frac{1}{2d^2} (r_1^2 + r_2^2) \right] \tag{58}$$

$$= 1 - \left[1 - \exp\left(- \frac{b^2}{2d^2} \right) \right]^2$$

$$\approx 2 \exp\left[- \frac{b^2}{2d^2} \right] \tag{59}$$

where

$$b = I_o^{-1}(k - 1) \tag{60}$$

The approximation leading to Eq. (59) stems from the fact that α is required to be small. Using Eq. (59), b can be found in terms of the allowable false-alarm probability per observation time, α^*. Thus

$$b \approx \sqrt{2d^2 \log(2/\alpha^*)} \tag{61}$$

This gives the threshold value k of Fig. 5

$$k = 1 + I_o\left[\sqrt{2d^2 \log(2/\alpha^*)} \right] \tag{62}$$

The detection probability can similarly be found, since the miss probability ($\beta = 1 - P_d$) is the probability that r_1, r_2 lies below the threshold if a signal is present, say, at ω_2.

$$Pd \doteq 1 - \int_o^b dr_1 \int_o^b dr_2 \frac{r_1 r_2}{d^4} \exp\left[- \frac{1}{2d^2} (r_1^2 + r_2^2 + d^4) \right] I_o(r_2) \tag{63}$$

$$= 1 - \left[1 - \exp\left(- \frac{b^2}{2d^2}\right)\right]\left[1 - Q\left(d, \frac{b}{d}\right)\right] \tag{64}$$

where Q(x,y) is the Q-function, given by

$$Q(x,y) = \int_y^\infty t\, e^{- \frac{(t^2 + x^2)}{2}} I_o(xt)\, dt \tag{65}$$

which has been tabulated by Marcum.[7]

A useful approximation is made in Eq. (64) by neglecting the exponential term as being much smaller than one and then using the value of b found in Eq. (61). This gives the detection probability in terms of the false-alarm probability and the detection index.

$$Pd \doteq Q\left(d, \sqrt{2 \log 2/\alpha^*} \right) \tag{66}$$

This function is plotted in Fig. 8 for several values of allowable false-alarm probability. Also presented in Fig. 8, for the purpose of comparison, are some results of Fig. 3 for the coherent case. For large values of signal-to-noise ratio, where the curves are very accurate, the incoherent detector yields detection probability curves that are parallel straight lines. This indicates that the detection probability follows a gaussian law, which may be seen by using the common approximation to the Q-function in Eq. (66), given by Rice [Ref. 8, p. 241]. It is important to realize that there is a constant loss between the coherent and incoherent results. In order to achieve the same detection probability with the incoherent detector as with the coherent detector, the detection index must be increased by adding about $d = .4$. For example, to achieve $\alpha = 10^{-4}$, $P_d = .9$, the coherent detector requires $d = 5.15$, whereas the incoherent detector requires $d = 5.6$. Analysis carried out in terms of known-phase signals would finally be altered by adjusting the required d. This difference could presumably be made up by increasing observation time. The attendant small increase in α would have little effect. This amount of required increase is found to increase slightly with higher false-alarm rates (equivalent to lower thresholds).

This result indicates that in the case of detecting a sine wave of unknown frequency in gaussian noise, the problem may be approached using coherent techniques, which are more convenient to work with, and then introduce some constant loss factor since knowledge of the phase is not available. In retrospect, this result is not so

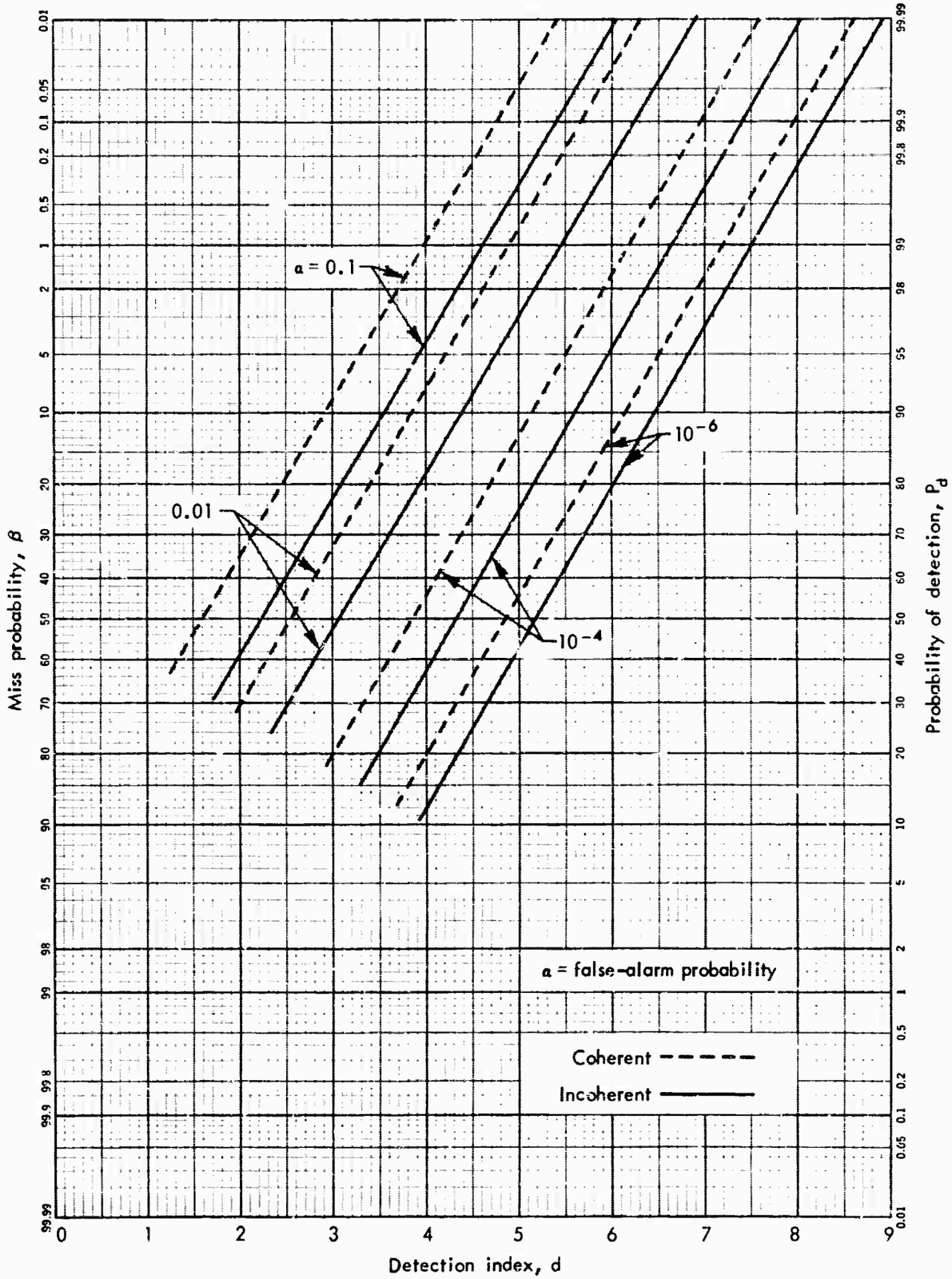

Fig. 8—Comparison of detectability of coherent and incoherent sine waves for case of two possible frequencies (m = 2)

surprising when it is considered how the detector forms the optimum likelihood ratio. It is well known that for a signal of known frequency in gaussian noise, the necessary increase in d is approximately .4 as well between the coherent and incoherent detectors. It seems reasonable that the same sort of behavior would continue to apply when a set of such variables is simply added in each case. It is useful, however, to know by how much this loss factor changes, as given above.

DETECTOR PERFORMANCE, m-FREQUENCY CASE

If the signal can appear at any one of m possible frequencies with, say, equal probability, the detector is that pictured in Fig. 5, and the decision curve satisfies

$$\sum_{i=1}^{m} I_o(r_i) = k \tag{67}$$

Again assuming that $|\omega_i - \omega_j| T >> 1$ if $\omega_i \neq \omega_j$ and $\omega_i T >> 1$ for all i,j so that the m quantities $I_o(r_i)$, i = 1, 2, ..., m are independent, the joint conditional density function of the m quantities may be formed, and these may be integrated over the m-dimensional decision space to obtain the false-alarm and detection probabilities. In a manner analogous to that in Section III, it may be demonstrated that the asymptotic approximation is valid for large values of d^2, and this approximation will be used here. Although the actual detector does form the likelihood ratio sum and compares it with the threshold, the computation uses the approximation that

the detector forms each of the m terms r_i and compares each of them with the threshold given by the asymptote, which is

$$r_i = I_o^{-1}\,[k - (m - 1)] \quad i = 1, 2, \ldots, m \tag{68}$$

Thus, the same combinatorial techniques may be used where the error probabilities associated with each quantity r_i are found. These then may be logically combined to obtain the overall error probabilities.

Each quantity r_i has the following distribution

$$P(r_i/H_o) = r_i/d^2 \exp(-r_i^2/2d^2) \tag{69}$$

$$P(r_i/H_i) = r_i/d^2 \exp[(-1/2d^2)(r_i^2 + d^4)]\, I_o(r_i) \tag{70}$$

The error probabilities may be formed exactly as done previously, with the result for each test quantity

$$\alpha_i = \exp(-g^2/2d^2) \tag{71}$$

$$\beta_i = 1 - Q(d, g/d) \tag{72}$$

where $g = I_o^{-1}[k - (m - 1)]$. Combining these for the m-frequency case, the overall false-alarm and detection probabilities become

$$\begin{aligned} \alpha &= 1 - (1 - \alpha_i)^m \approx m\alpha_i \\ &\doteq m \exp[-g^2/2d^2] \end{aligned} \tag{73}$$

$$\beta = \beta_i(1 - \alpha_i)^{m-1} \approx \beta_i$$

so that

$$P_d \doteq 1 - \beta_i = Q(d, g/d) \tag{74}$$

Solving Eqs. (73) and (74) for P_d in terms of α^*, the allowable false-alarm probability, the detection probability

$$P_d = Q\left(d, \sqrt{2 \log \frac{m}{\alpha^*}}\right) \tag{75}$$

Curves of P_d versus d for various values of m and for $\alpha = 10^{-2}$ and 10^{-6} are given in Fig. 9, along with some of the coherent detector results of Fig. 4 for comparison. It is seen that the curves are straight lines, indicating that the detectability follows a gaussian law as is expected from the normal approximation to the Q-function. Also, it is seen that if the number m of possible frequencies at which the signal may appear is doubled, an increase in d of between .1 and .2 is required in order to achieve the same detection probability. This very slight loss is encouraging since in practice the exact frequency would not be known, and many narrow-band filters would have to be built in order to cover the entire band of interest.

The results seem intuitively satisfying, since in Eq. (75) it is seen that the lack of knowledge about the exact signal frequency requires that the thresholds be set slightly higher than in the known frequency case (m = 1). Since a filter is used for each possible frequency, and there are m parallel detectors contributing possible false alarms, a higher threshold will maintain the desired false-alarm rate. Also, the appearance of the simple factor d in Eq. (75) indicates that if a signal is present in one of the m filters, it alone is significant in causing a detection. The approximation of Eq. (74) shows this by neglecting the very small contribution to

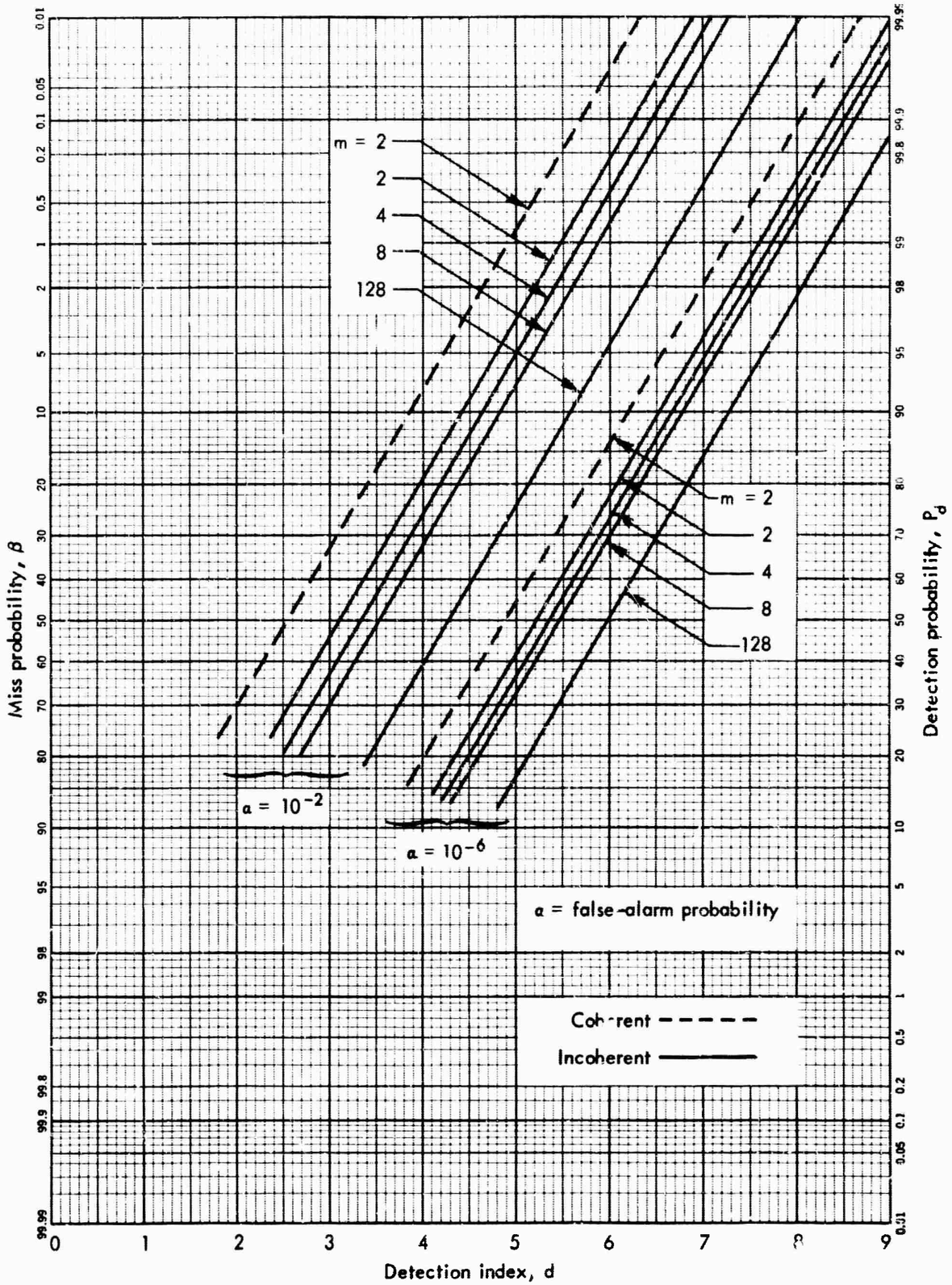

Fig. 9—Comparison of detectability of incoherent sinusoid for case of m possible frequencies with detectability of coherent sinusoid for case of two possible frequencies (m = 2)

a target-present decision from noise false alarms. It is seen that the optimum detector, by passing the filtered signal through a Bessel function device, greatly accentuates the large signals and depresses the small signals. This fact causes the single large signal--if present--to predominate.

V. CONCLUSIONS

The results of the above analysis indicate that it is not necessary to work in terms of unknown phase detection when considering unknown frequency in order to be realistic. For the case of a finite number of known frequencies at which the signal may appear, it is apparent that any real situation may be approached as if the phase were indeed known and thus work with gaussian statistics. This greatly simplifies the analysis, especially for a large number of possible frequencies. An adjustment is made at the end of the analysis to account for the actual ignorance of the signal phase, but this adjustment is quite constant for many different situations, thereby allowing accurate final results.

It is seen that the optimum detector for both the coherent and incoherent cases is a nonlinear device, which acutely accentuates large received signals. This seems quite reasonable under the circumstances, for the detector is testing the sum of a large number of random variables, and unless the detector weighted these in some manner that drew attention to the strongest member, or equivalently suppressed the smaller members, the false-alarm rate would be very high, necessitating a higher threshold setting which would reduce the detection capability.

By means of the decision plane geometry it is seen that, although the optimum detector actually tests the sum of the filter outputs against a threshold, the system may be analyzed as if each filter output were separately tested against the threshold. This is, of

course, a result again of the emphasis placed on large signals. The system then becomes one of a band-splitting type which divides the frequency band of concern into a set of small independent bands and interrogates each for the presence of a signal. The approximation of considering the optimum detector as a band-splitting detector, which is made clear through the use of the geometric approach, is very g for large output signal-to-noise ratios. It is seen from the d n-plane representation just how the optimum detector approaches the situation of m approximately orthogonal signals in noise. The asymptotic approximation finally isolates each filter output, permitting m independent decisions.

Even though the power levels of the signal and noise may be very unfavorable at the hydrophone, a long integration time will increase the signal-to-noise ratio to a useful value. This requires that the noise level and signal level be constant for the duration of the observation interval. In practice, the duration of each observation interval will be limited by the noise nonstationarity and/or the time of passage of the target.

The problem of unknown noise level has been shown by Tuteur[9] to be of critical importance in an actual detection situation. He has considered the effect of noise uncertainty on the detectability of submarines by means of their emission of broadband signals and has demonstrated that unreasonable detection ranges result if noise uncertainty is ignored. He suggests a long-term average-power measurement of the noise level, which would include and presumably "swamp out" the short-term fluctuation due to the target's own wide-

band noise as it passed by the hydrophone, as a means of estimating actual noise level. This technique is intuitively appealing in the present study also, since the sine wave power will have little effect on the long-term wideband noise power estimate. There is need for further analysis which considers the detection of both the wideband noise and the sine wave signals simultaneously, especially in light of the critical nature of the results for noise level uncertainty.

Appendix A

PROBABILITY DISTRIBUTION OF THE TEST QUANTITIES

It is required to find the joint conditional probability density functions for the test quantities

$$x_1 = \log L_1 = -\frac{1}{2}\,\underline{s}_1'\,\underline{\underline{K}}^{-1}\,\underline{s}_1 + \underline{s}_1'\,\underline{\underline{K}}^{-1}\,\underline{v} \qquad \text{(A-1)}$$

$$x_2 = \log L_2 = -\frac{1}{2}\,\underline{s}_2'\,\underline{\underline{K}}^{-1}\,\underline{s}_2 + \underline{s}_2'\,\underline{\underline{K}}^{-1}\,\underline{v} \qquad \text{(A-2)}$$

where the quantities are as defined in Section III. Since the only random variable appearing in these expressions is the vector $\underline{v}$, which is jointly gaussian (in n-dimensions), and since the quantities x_1, x_2 are formed by linear superpositions of these gaussian variables, x_1 and x_2 are gaussian random variables. Hence it only remains to find their mean and variance under the three hypotheses, H_o, H_1, and H_2, as defined in Section III.

Let the notation

$$\langle\ \rangle_{H_o} \qquad \text{(A-3)}$$

indicate the statistical average of the quantity in brackets under the hypothesis H_o, and similarly for H_1 and H_2. If no subscript appears, then $\underline{v}$ has already been changed to its component parts, and the average is that over the noise portion. It is clear that these hypotheses imply

$$H_o : \quad v(t) = n(t)$$

$$H_1 : \quad v(t) = n(t) + s_1(t) \tag{A-4}$$

$$H_2 : \quad v(t) = n(t) + s_2(t)$$

Thus, using standard matrix techniques, the conditional averages are

$$\left\langle x_1 \right\rangle_{H_o} = -\frac{d^2}{2} + \left\langle \underline{s}_1' \underline{K}^{-1} \underline{v} \right\rangle_{H_o}$$

$$= -\frac{d^2}{2} + \underline{s}_1' \underline{K}^{-1} \left\langle \underline{v} \right\rangle_{H_o} \tag{A-5}$$

$$= -\frac{d^2}{2}$$

since the noise has zero mean, and where, as shown in Section III

$$\frac{d^2}{2} = \frac{1}{2} \underline{s}_1' \underline{K}^{-1} \underline{s}_1 = \frac{1}{2} \underline{s}_2' \underline{K}^{-1} \underline{s}_2 \tag{A-6}$$

$$\left\langle x_1 \right\rangle_{H_1} = -\frac{d^2}{2} + \left\langle \underline{s}_1' \underline{K}^{-1} (\underline{s}_1 + n) \right\rangle_{H_1}$$

$$= -\frac{d^2}{2} + d^2 + \underline{s}_1' \underline{K}^{-1} \left\langle \underline{n} \right\rangle \tag{A-7}$$

$$= +\frac{d^2}{2}$$

$$\left\langle x_1 \right\rangle_{H_2} = -\frac{d^2}{2} + \left\langle \underline{s}_1' \underline{K}^{-1} (\underline{s}_2 + n) \right\rangle_{H_1}$$

$$= -\frac{d^2}{2} + \underline{s}_1' \underline{K}^{-1} \underline{s}_2 \tag{A-8}$$

$$= -\frac{d^2}{2}$$

In Eq. (A-8), $\underline{s}_1' \underline{K}^{-1} \underline{s}_2 \doteq 0$. This is so because this term indicates the cross-correlation of two sine waves of different frequencies. In particular, using the conditions of Eq. (16), where the noise is assumed white, there results (provided that $|\omega_1 - \omega_2| T >> 1$)

$$\underline{s}_1' \underline{K}^{-1} \underline{s}_2 = \frac{1}{N_o \Omega} \sum_{j=1}^{n} P^2 \cos(\omega_i t_j + \varphi_1) \cos(\omega_2 t_j + \varphi_2)$$

$$\approx \frac{2}{N_o} \int_o^T P^2 \cos(\omega_1 t + \varphi_1) \cos(\omega_2 t + \varphi_2) \, dt \qquad \text{(A-9)}$$

$$\approx 0$$

This is not an exact relation, except when $|f_1 - f_2|$ is a multiple of 1/T cps, but the term in Eq. (A-9) does not increase with time for reasonably large T, whereas the term $-\frac{d^2}{2}$ grows linearly with time. Thus, the cross-correlation term becomes negligible with respect to the $\frac{d^2}{2}$ term for large observation times.

To compute the variances of $x_1 = \log L_1$

$$\text{var}_{H_o}[x_1] = \left\langle \left(-\frac{d^2}{2} + \underline{s}_1' \underline{K}^{-1} \underline{v} \right)^2 \right\rangle_{H_o} - \frac{1}{4} d^4$$

$$= \left\langle \underline{s}_1' \underline{K}^{-1} \underline{v} \, \underline{v}' \underline{K}^{-1} \underline{s}_1 \right\rangle_{H_o} - \underline{s}_1' \underline{K}^{-1} \underline{s}_1 \, \underline{s}_1' \underline{K}^{-1} \left\langle \underline{v} \right\rangle_{H_o}$$

$$= \underline{s}_1' \underline{K}^{-1} \left\langle \underline{v} \, \underline{v}' \right\rangle_{H_o} \underline{K}^{-1} \underline{s}_1 \qquad \text{(A-10)}$$

$$= \underline{s}_1' \underline{K}^{-1} \underline{K} \, \underline{K}^{-1} \underline{s}_1$$

$$= \underline{s}_1' \underline{K}^{-1} \underline{s}_1$$

$$= d^2$$

$$\text{var}_{H_1}[x_1] = \left\langle \left(-\frac{d^2}{2} + \underline{s}_1' \underline{K}^{-1}(\underline{s}_1 + \underline{n}) \right)^2 \right\rangle - \frac{1}{4} d^4$$

$$= \left\langle \left(+\frac{d^2}{2} + \underline{s}_1' \underline{K}^{-1} \underline{n} \right)^2 \right\rangle - \frac{1}{4} d^4$$

$$= \frac{d^4}{4} + \underline{s}_1' \underline{K}^{-1} \underline{s}_1 \, \underline{s}_1' \underline{K}^{-1} \left\langle \underline{n} \right\rangle + \underline{s}_1' \underline{K}^{-1} \left\langle \underline{n} \, \underline{n}' \right\rangle \underline{K}^{-1} \underline{s}_1 - \frac{d^4}{4}$$

$$= \underline{s}_1' \underline{K}^{-1} \underline{s}_1 \qquad \text{(A-11)}$$

$$= d^2$$

$$\text{var}_{H_2}[x_1] = \left\langle \left(-\frac{d^2}{2} + \underline{s}_1' \underline{K}^{-1}(\underline{s}_2 + \underline{n}) \right)^2 \right\rangle - \frac{d^2}{4}$$

$$= -\underline{s}_1' \underline{K}^{-1} \underline{s}_1 \, \underline{s}_1' \underline{K}^{-1} \underline{s}_2 + (\underline{s}_1' \underline{K}^{-1} \underline{s}_2)^2 + \underline{s}_1' \underline{K}^{-1} \left\langle \underline{n} \, \underline{n}' \right\rangle \underline{K}^{-1} \underline{s}_1$$

$$= \underline{s}_1' \underline{K}^{-1} \underline{s}_1 \qquad \text{(A-12)}$$

$$= d^2$$

The same results are obtained when $x_2 = \log L_2$ is averaged over the hypotheses, since x_1 and x_2 are similarly distributed. It still remains to find the correlation between x_1 and x_2. The normalized correlation coefficient is

$$\frac{1}{d^2}\left\langle \left(x_1 + \frac{d^2}{2}\right)\left(x_2 + \frac{d^2}{2}\right)\right\rangle_{H_o} = \frac{1}{d^2}\left\langle \underline{s}_1' \underline{K}^{-1} \underline{v}\, \underline{v}' \underline{K}^{-1} \underline{s}_2 \right\rangle_{H_o}$$

$$= \frac{1}{d^2} \underline{s}_1' \underline{K}^{-1} \left\langle \underline{v}\, \underline{v}' \right\rangle_{H_o} \underline{K}^{-1} \underline{s}_2 \qquad \text{(A-13)}$$

$$= \frac{1}{d^2} \underline{s}_1' \underline{K}^{-1} \underline{s}_2$$

$$\approx 0$$

Thus, x_1 and x_2 are uncorrelated and consequently independent. The joint distribution can then be expressed according to the results found here, and these are given in Eqs. (21), (22) and (23).

Appendix B

JOINT DENSITY FUNCTION OF THE ENVELOPES OF TWO CORRELATORS

In the following derivation, the input is assumed to be a stationary gaussian noise process with the spectrum level $N_o/2$ volts^2/cps and band limited to $(-\Omega, \Omega)$. It is assumed that $T >> 1/\Omega$. Thus, the noise may be considered as being white, and the following may be used for the input autocorrelation function

$$R_n(\tau) = \frac{N_o}{2} \delta(\tau) \tag{B-1}$$

where $\delta(x)$ is defined by

$$\int_{-\infty}^{\infty} f(x)\ \delta(x - a)\ dx = f(a) \tag{B-2}$$

and $f(x)$ is any function continuous at $x = a$.

As discussed in Section IV, the optimum detector must form the two quantities defined by

$$I_1 \equiv \frac{2P}{N_o} \int_o^T v(t) \cos \omega_1 t\ dt$$

and (B-3)

$$I_2 \equiv \frac{2P}{N_o} \int_o^T v(t) \sin \omega_1 t\ dt$$

for the optimum detection of a sine wave at frequency ω_1 rad/sec. It then forms the envelope $_1$ using these quantities according to Eq. (36). It was shown there that the correlations performed in Eq. (B-3) could be carried out by a "narrow-band" filter centered at ω_1, as described by Eq. (37). In the following, the terms "filter"

and "correlator" will be used interchangeably, referring always to the device that performs the operations of Eq. (36).

Considering further a second filter centered at ω_2

$$I_3 = \frac{2P}{N_o} \int_o^T v(t) \cos \omega_2 t \, dt$$

and

$$I_4 = \frac{2P}{N_o} \int_o^T v(t) \sin \omega_2 t \, dt \qquad \text{(B-4)}$$

Under the hypothesis H_o that the input v(t) consists of noise alone, the outputs I_1, I_2, I_3 and I_4 are each the result of linear processing of a gaussian process and hence are all jointly normal random variables. It is only necessary to find the first and second moments for each in order to specify the joint distribution completely.

Each quantity I_i has zero mean since n(t) has zero mean. The second moments are calculated as follows

$$\begin{aligned}
\overline{I_1^2} &= \left(\frac{2P}{N_o} \right)^2 \int_o^T d\tau \int_o^T d\sigma \, \overline{n(\tau)\, n(\sigma)} \cos \omega_1 \tau \cos \omega_1 \sigma \\
&= \left(\frac{2P}{N_o} \right)^2 \int_o^T d\tau \int_o^T d\sigma \, \frac{N_o}{2} \delta(\tau - \sigma) \cos \omega_1 \tau \cos \omega_1 \sigma \\
&= \frac{2P^2}{N_o} \int_o^T d\tau \cos^2 \omega_1 \tau \qquad \text{(B-5)} \\
&\doteq \frac{P^2 T}{N_o} \equiv \psi
\end{aligned}$$

The result is not exact, but as T increases, the rapidly oscillating portion of the integrand contributes very little to the variance. Similarly, it is easily shown that

$$\overline{I_2^2} = \overline{I_3^2} = \overline{I_4^2} = \frac{P^2 T}{N_o} \equiv \psi \tag{B-6}$$

The covariances are calculated in a similar manner.

$$\overline{I_1 I_2} = \left(\frac{2P}{N_o} \right)^2 \int_o^T d\tau \int_o^T d\sigma \, \overline{n(\tau)\, n(\sigma)} \cos \omega_1 \tau \sin \omega_1 \sigma$$

$$= \frac{2P^2}{N_o} \int_o^T \cos \omega_1 \tau \sin \omega_1 \tau \, d\tau \tag{B-7}$$

$$= \frac{P^2}{N_o} \int_o^T \sin 2\omega_1 \tau \, d\tau \equiv \mu_{12}$$

This term does not increase with time, and consequently as T increases, it will become negligible with respect to the variances having the value P^2T/N_o. It is thus set to zero at this point.

$$\overline{I_1 I_3} = \frac{2P^2}{N_o} \int_o^T \cos \omega_1 \tau \cos \omega_2 \tau \, d\tau$$

$$= \frac{P^2 T}{N_o} \left[\frac{\sin(\omega_2 - \omega_1)\, T}{(\omega_2 - \omega_1)\, T} + \frac{\sin(\omega_2 + \omega_1)\, T}{(\omega_2 + \omega_1)\, T} \right] \tag{B-8}$$

$$\approx \frac{P^2 T}{N_o} \frac{\sin(\omega_2 - \omega_1)\, T}{(\omega_2 - \omega_1)\, T} \equiv \mu_{13}$$

The approximation in Eq. (B-8) assumes that the frequencies ω_2 and ω_1 are close enough together so that $(\omega_2 + \omega_1) >> |\omega_2 - \omega_1|$, thus making the sum frequency term above small with respect to the difference frequency term. If this is not the case and instead $(\omega_2 + \omega_1) \approx |\omega_2 - \omega_1|$, then

$$\overline{I_1 I_3} \doteq \frac{P^2 T}{N_o} \frac{2 \sin \omega_2 T}{\omega_2 T} \qquad (\text{say } \omega_2 > \omega_1) \tag{B-9}$$

The results will be the same in either case, but the interesting case of ω_2 close to ω_1 will be considered here, and Eq. (B-8) will be used. Similarly, the other moments are easily obtained.

$$\overline{I_2 I_4} \doteq \mu_{13} \ , \ \overline{I_3 I_4} = \frac{P^2}{N_o} \int_o^T \sin 2\omega_2 \tau \, d\tau \equiv \mu_{34} \approx 0$$

$$\overline{I_1 I_4} \doteq \frac{P^2 T}{N_o} \frac{1 - \cos(\omega_2 - \omega_1) T}{(\omega_2 - \omega_1) T} \equiv \mu_{14} = \overline{-I_2 I_3} \tag{B-10}$$

These quantities define a symmetrical covariance matrix M like that of Rice [Ref. 8, p. 215], which may be inverted to form the information matrix M^{-1}

$$M^{-1} = \frac{1}{A} \begin{bmatrix} \psi & 0 & -\mu_{13} & -\mu_{14} \\ 0 & \psi & \mu_{14} & -\mu_{13} \\ -\mu_{13} & \mu_{14} & \psi & 0 \\ -\mu_{14} & -\mu_{13} & 0 & \psi \end{bmatrix} \tag{B-11}$$

where

$$\psi = \frac{P^2 T}{N_o} \qquad \text{and} \qquad A = \psi^2 - (\mu_{13}^2 + \mu_{14}^2) = \psi^2 - \psi_{12}^2 \tag{B-12}$$

By comparing the variances and the cross moments defined above, it is readily seen that as long as $|\omega_2 - \omega_1| T >> 1$, $\omega_1 T >> 1$, and $\omega_2 T >> 1$, all of the cross moments will become negligible with respect to ψ for large T. Thus, M^{-1} reduces to a diagonal matrix indicating that the random variables I_i are independent, and $A \doteq \psi^2$ results.

Thus, for the conditional joint density function under the hypothesis H_o (under which all variables have zero mean)

$$p(I_1, I_2, I_3, I_4 / H_o) = \frac{1}{4\pi^2 \psi^2} \exp\left[- \frac{1}{2\psi} (I_1^2 + I_2^2 + I_3^2 + I_4^2) \right] \tag{B-13}$$

The standard transformation may be made to the Rayleigh distribution for the envelopes $r_1 = \sqrt{I_1^2 + I_2^2}$ and $r_2 = \sqrt{I_3^2 + I_4^2}$ [Ref. 8, p. 214], using

$$\begin{aligned} I_1 &= r_1 \cos \theta_1 & I_3 &= r_2 \cos \theta_2 \\ I_2 &= r_1 \sin \theta_1 & I_4 &= r_2 \sin \theta_2 \end{aligned} \tag{B-14}$$

Using standard techniques for transformations of random variables [Ref. 3, p. 31], the following is obtained for the conditional joint distribution of the envelopes r_1, r_2, from Eq. (B-13)

$$p(r_1, r_2 / H_o) = \frac{r_1 r_2}{d^4} \exp\left[- \frac{1}{2d^2} (r_1^2 + r_2^2) \right] \tag{B-15}$$

where, using ψ of Eq. (B-12)

$$d^2 = \frac{P^2 T}{N_o} \tag{B-16}$$

as in the coherent case. Also, this form for r_1, r_2 is seen to be exactly that for the r_1 of Eq. (36).

When a sine wave is present at the input of the form $P \cos(\omega_2 t + \xi)$ for any angle ξ, it is clear that the quantities I_3 and I_4 will have their means shifted from zero to the values

$$\overline{I_3(T)} = \frac{2P}{N_o} \int_o^T P \cos(\omega_2 t + \xi) \cos \omega_2 t \, dt =$$

$$\frac{P^2 T}{N_o} \left[\cos \xi + \frac{\sin(2\omega_2 T + \xi) - \sin \xi}{2\omega_2 T} \right] \tag{B-17}$$

$$\approx d^2 \cos \xi \qquad \text{if } \omega_2 T >> 1$$

$$\overline{I_4(T)} = \frac{2P}{N_o} \int_o^T P \cos(\omega_2 t + \xi) \sin \omega_2 t \, dt =$$

$$\frac{P^2 T}{N_o} \left[- \sin \xi + \frac{\cos \xi - \cos(2\omega_2 T + \xi)}{2\omega_2 T} \right] \tag{B-18}$$

$$\approx -d^2 \sin \xi \qquad \text{if } \omega_2 T >> 1$$

Due to signal alone, the envelope r_2 will have a value of approximately d^2. If the above mean values are used in Eq. (B-13) and the same transformation as in Eq. (B-14) is used, the joint distribution

of r_1, r_2 may be easily obtained [Ref. 8, pp. 214, 238]. Here only the final result is given

$$p(r_1,r_2/H_2) = \frac{r_1 r_2}{d^4} \exp\left[-\frac{1}{2d^2}(r_1^2 + r_2^2 + d^4)\right] I_o(r_2) \qquad \text{(B-19)}$$

This completes the derivation of the envelope statistics, but a slight extension is now made, both as a matter of interest and also because it yields a useful measure of filter output dependence. The joint distribution of the envelopes r_1 and r_2 when the dependence is not negligibly small is given here. Thus, starting from the information matrix of Eq. (B-11), μ_{13} and μ_{14} are retained throughout, letting only μ_{12} and μ_{34} be zero, which is reasonable in light of their definitions. The following result may be obtained in a manner similar to Rice's derivation of the autocorrelation function for a filter output [Ref. 8, p. 216] but extends the analysis to the case when a sine wave is present at frequency ω_2. The dependence between r_1 and r_2 is seen to occur as $\psi_{12}^2 = \mu_{13} + \mu_{14}^2$; that is, r_1 and r_2 are completely independent only if $\psi_{12} = 0$.

The result is as follows: For two envelopes r_1 and r_2 under hypothesis H_2, assuming only that μ_{12} and μ_{34} in Eq. (B-11) are small

$$p(r_1,r_2/H_2) = \frac{r_1 r_2}{2\pi d^4 \sigma} \int_o^{2\pi} d\theta \exp\left(\frac{-r_1^2}{2d^2\sigma}\right) \exp\left[-\frac{1}{2\sigma}\beta^2(\theta)\right]$$

$$I_o\left[\frac{\sqrt{1-\sigma}}{\sigma}\frac{r_1}{d}\beta(\theta)\right] \qquad \text{(B-20)}$$

where

$$\sigma = 1 - \frac{\psi_{12}^2}{d^4} \quad , \quad \psi_{12}^2 = \mu_{13}^2 + \mu_{14}^2 \tag{B-21}$$

and

$$\beta^2(\theta) = \frac{r_2^2}{d^2} + d^2 - 2r_2 \cos\theta \tag{B-22}$$

A closed-form expression for this was not found, although numerical techniques could be used to evaluate it.

Under the hypothesis H_o of noise only, the only change is that $\beta^2(\theta) = r_2^2/d^2$, which permits a closed-form evaluation

$$p(r_1, r_2/H_o) = \frac{r_1 r_2}{d^4 \sigma} \exp\left[-\frac{1}{2d^2\sigma}(r_1^2 + r_2^2)\right] I_o\left[\frac{\sqrt{1-\sigma}}{\sigma}\frac{r_1 r_2}{d^2}\right] \tag{B-23}$$

which agrees with Bendat [Ref. 6, p. 308] and provides a convenient check. If $\psi_{12} = 0$, then $\sigma = 1$, and it is easily seen that r_1 and r_2 become independent, leading to Eqs. (B-15) and (B-19) under H_o and H_2 respectively.

Appendix C

AUTOCORRELATION FUNCTION FOR THE ACTUAL NARROW-BAND FILTER

Consider the output of the narrow-band filter with impulse response as in Eq. (49), when the filter is connected only during (0,T). The scaling factor $2P/N_oK_1$ is added by means of an amplifier in order to concur with Eq. (50)

$$h_T(\tau) = \begin{cases} K_1 e^{-\epsilon\tau}\cos(\omega_i\tau + \varphi) & 0 \le \tau \le T \\ 0 & \text{Otherwise} \end{cases} \qquad \text{(C-1)}$$

The input process to the filter is a stationary white noise process of the level $N_o/2$ volts^2/cps. The noise could as well be band-limited to a band $(-\Omega, \Omega)$; for as long as the passband of the filter is narrow with respect to this band, the noise could still be assumed white.

The output correlation function is given by Lee [Ref. 5, p. 332]

$$R(\tau) = \int_{-\infty}^{\infty} h_T(v)\, dv \int_{-\infty}^{\infty} h_T(\sigma)\, R_i(\tau + v - \sigma)\, d\sigma \qquad \text{(C-2)}$$

where the input correlation function $R_i(\tau)$ is given by Eq. (B-1) and equals $\frac{N_o}{2}\,\delta(\tau)$. Thus

$$R(\tau) = \left(\frac{4P^2}{N_o^2}\right) \int_o^T e^{-\epsilon v}\cos(\omega_i v + \varphi)\, dv \int_o^T e^{-\epsilon\sigma}\cos(\omega_i\sigma + \varphi)\, \frac{N_o}{2}\,\delta(\tau + v - \sigma)\, d\sigma \qquad \text{(C-3)}$$

$$= \frac{2P^2}{N_o} \int_o^T e^{-\epsilon(2v+\tau)}\cos(\omega_i v + \varphi)\cos[\omega_i(\tau + v) + \varphi]\, dv \qquad \text{(C-4)}$$

if $(\tau + v)$ lies in $(0,T)$

and equals zero if $\tau + \upsilon$ does not lie in (0, T). This restriction on $\tau + \upsilon$ requires that for a given value of τ, the range of υ is $(-\tau, T - \tau)$; and τ is also restricted to (0, T). This sets the upper limit of the integral

$$R(\tau) = \frac{P^2}{N_o} e^{-\epsilon\tau} \int_o^{T-\tau} e^{-2\epsilon\upsilon} [\cos \omega_i \tau + \cos(2\omega_i \upsilon + 2\varphi + \omega_i \tau)] \, d\upsilon \qquad (C\text{-}5)$$

if $\tau < T$, and zero otherwise.

The rapidly oscillating portion of the integrand may be neglected as it contributes very little to $R(\tau)$, provided $2\omega_i |T - \tau| >> 1$. Thus

$$R(\tau) = \frac{P^2}{N_o} e^{-\epsilon\tau} \cos \omega_i \tau \int_o^{T-\tau} e^{-2\epsilon\upsilon} \, d\upsilon \qquad (C\text{-}6)$$

$$= \frac{P^2}{N_o} e^{-\epsilon\tau} \cos \omega_i \tau \left[\frac{1}{2\epsilon} \right] \left[1 - e^{-2\epsilon\tau(T-\tau)} \right] \qquad (C\text{-}7)$$

and the variance is given by R(0) as

$$\psi_{fil} = \frac{P^2}{2\epsilon N_o} \left[1 - e^{-2\epsilon T} \right] \qquad (C\text{-}8)$$

For a sine wave input to the circuit, the output of the filter at time T may be found in a manner similar to that of Eqs. (B-17) and (B-18) of Appendix B. The result is that the envelope has the value

$$r(T) = \frac{P^2}{N_o \epsilon} \left[1 - e^{-\epsilon\tau} \right] \qquad (\text{for } 2\omega_i T >> 1) \qquad (C\text{-}9)$$

Consider the case where $\epsilon T << 1$; that is, where the filter is very narrow band relative to the observation time. Then Eq. (C-8) reduces to

$$\psi_{fil} \doteq \frac{P^2 T}{N_o} \qquad (\varepsilon T << 1) \qquad \text{(C-10)}$$

and Eq. (C-9) becomes

$$r(T) \doteq \frac{P^2 T}{N_o} \qquad (\varepsilon T << 1) \qquad \text{(C-11)}$$

REFERENCES

1. Helstrom, C. W., Statistical Theory of Signal Detection, Pergamon Press, London, 1960.

2. Levesque, A. H., Optimal Detection of a Coherent Sinusoid with Unknown Frequency, Yale University, Report No. 15, Electric Boat Research (53-00-10-0231), June 1964.

3. Davenport, W. B. and W. L. Root, Random Signals and Noise, McGraw-Hill Book Co., Inc., New York, 1958.

4. Jahnke, E. and F. Emde, Tables of Functions, Dover Publications, New York, 1945.

5. Lee, Y. W., Statistical Theory of Communication, J. Wiley and Sons, Inc., New York, 1960.

6. Bendat, J. S., Principles and Applications of Random Noise Theory, J. Wiley and Sons, Inc., New York, 1958.

7. Marcum, J. I., Table of Q-Functions, The RAND Corporation, RM-339, January 1950.

8. Rice, S. O., Mathematical Analysis of Random Noise, Dover Publications, New York, 1954.

9. Tuteur, F. B., Some Aspects of the Detectability of Broadband Sonar Signals by Nondirectional Passive Hydrophones, The RAND Corporation, RM-4578-ARPA, June 1965.

DOCUMENT CONTROL DATA

1. ORIGINATING ACTIVITY	2a. REPORT SECURITY CLASSIFICATION
THE RAND CORPORATION	UNCLASSIFIED
	2b. GROUP

3. REPORT TITLE

DETECTION OF SONAR SINUSOIDS OF UNKNOWN FREQUENCY AND KNOWN OR U KNOWN PHASE

4. AUTHOR(S) (Last name, first name, initial)

Hill, Jr., F. S.

5. REPORT DATE	6a. TOTAL NO. OF PAGES	6b. NO. OF REFS.
December 1965	79	9

7. CONTRACT or GRANT NO.	8. ORIGINATOR'S REPORT NO.
SD-79	RM-4809-ARPA

9a. AVAILABILITY/LIMITATION NOTICES	9b. SPONSORING AGENCY
DDC 1	Advanced Research Projects Agency

10. ABSTRACT

A consideration of the problem of detecting a constant sine wave of unknown frequency and amplitude in gaussian noise. The Memorandum assumes that the sinusoid may appear at any one of a finite number of known frequencies, and the probability of its occurrence at each of these frequencies is assumed to be equal. Two cases are treated: the first assumes that, although the frequency is not known, the phase of the signal is known, thus allowing coherent detection; the second acknowledges that the initial phase could not be known, and an analysis of the incoherent detector is made. The results indicate that the difference between the two cases is small and quite predictable. Thus, it can be assumed that, in studies of this kind, the initial phase is known, the gaussian character of the quantities that arise may be retained, and the answers can be adjusted to account for the actual lack of knowledge concerning the phase.

11. KEY WORDS

Sonar
Detection
Gaussian noise
Radar
Signals